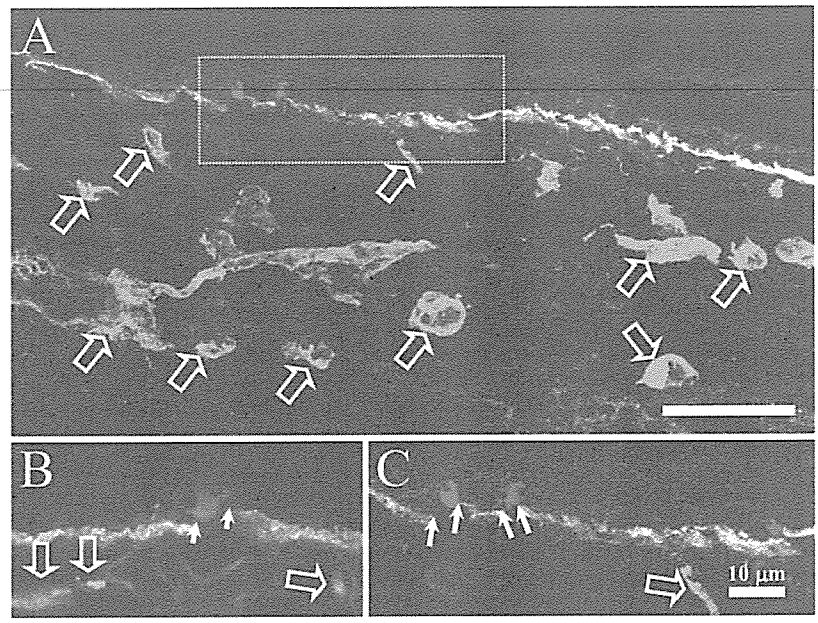

Figure 2 Reduced laminin 10 (green, FITC) and laminin 5 (red, Texas Red) labeling below the melanocyte marker TMH-1 (blue, CY-5) of normal adult control skin. Both laminin 5 and the α5 chain colocalize (orange color) within the dermal–epidermal junction (**A**) and both are expressed only weakly or are absent beneath melanocytes (**B,C**, in blue, see white arrows). The α5 chain of laminins 10/11 together with laminin 5 is not expressed beneath melanocytes (**A–C**, white arrows) but does show a distinct, strong expression pattern that includes dermal vessels (**A–C**, open arrows). Bar = 25 μm; Inset **C** = 10 μm.

characteristic pattern of staining along the majority of the follicles, for both laminin 5 (bracketed area in Figure 3A) and the laminin α5 chain (brackets and dotted line in Figures 3B and 3D). The laminin β1 and γ1 chains also showed this staining pattern (data not shown). There was no staining for the β2 chain in the hair follicle (data not shown). The dermal–epidermal junction of the bulge region stained for both α3 and the α5 chains (Figures 3A and 3B, Bu) and the α5 chain also stained the erector pili muscle (Figure 3C, EP).

Confocal Fluorescence Microscopy of Epidermolysis Bullosa Skin

The expression of laminins 5 (γ2 chain), 10 (all chains), and 11 (β2 chain) in patients with different forms of EB

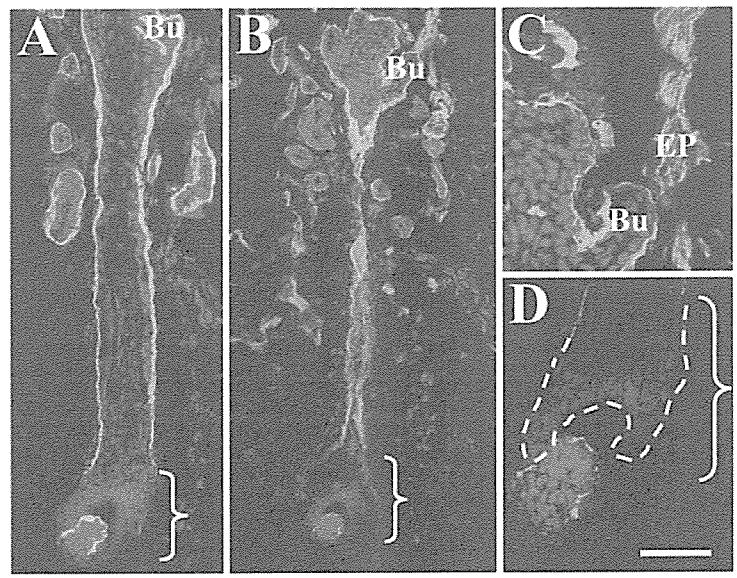

Figure 3 Indirect immunofluorescence shows a typical hemidesmosomal (HD) component-like expression pattern of the laminin α5 chain in late anagen human hair follicles. A previous scalp hair follicle immunohistochemical study (Akiyama et al. 1995) demonstrated a specific staining pattern for many HD-anchoring filament-associated components including laminin 5. In our study, both laminin-5 polyclonal staining (**A**) and the laminin α5 chain (**B**, 4C7) showed characteristic bright patterns along the epidermal proximal hair shaft including the bulge region (**B,C**, Bu) but progressively weaker staining toward the hair bulb (**D**, bracketed areas) with staining becoming brighter again higher up the hair shaft. Laminin α5 chain staining was present in the shaft (**B**) bulge region (**B,C**) and the apical tip of the hair bulb matrix (**D**). Laminin β1 and γ1 chains showed similar staining to the α5 chain (data not shown). No laminin β2 chain staining was detected in the hair follicle (data not shown). Bar = 25 μm.

was compared. In both control (Figure 4A) and all of the EB subtypes (Figures 4B–4H), α5, β1, β2, and γ1 chain expression was detectable. Laminin expression was weak in areas of split skin particularly in HJEB with defects in laminin 5 (α5 chain, Figures 4B and 4C, respectively, asterisks show the split area) (Uitto and Pulkkinen 2001). The reduction in α5 and β2 chain expression in HJEB patients, particularly over split skin,

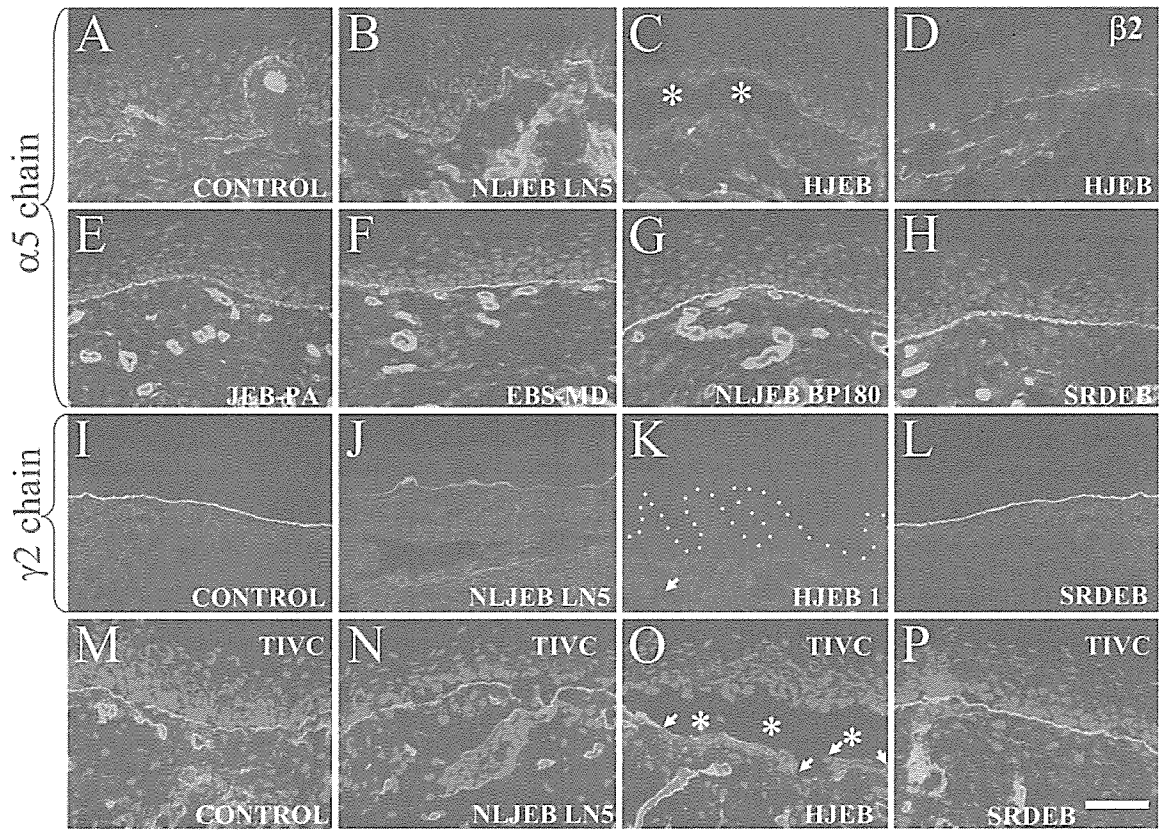

Figure 4 Laminin α5 and β2 chains are expressed beneath the epidermis in epidermolysis bullosa (EB) skin but are focally reduced in split lethal Herlitz junctional EB (HJEB) skin. The laminin α5 chain in control skin showed linear fluorescence along the dermal–epidermal junction and in dermal blood vessels (**A**). However, in non-lethal (**B**) and HJEB skin (**C,D**), the laminin α5 and β2 chains showed reductions in dermal–epidermal junction staining, especially where areas of skin had become separated (**C**, asterisks). This effect was due to antigen degradation in HJEB skin during skin separation as demonstrated by reduced collagen IV staining (**O**, arrows:) over the split areas (**O**, asterisks), whereas control skin (**M**), non-lethal junctional EB (NLJEB) (**N**) and dystrophic EB skin (**P**) showed bright linear collagen IV staining, respectively. The presence of α5 and β2 chain staining in intact EB skin demonstrates that these chains are independently synthesized and maintained even in the presence of other defective basement membrane components. All other cases of EB showed normal staining for the laminin α5 chain (and β2 chain, not shown), including junctional EB associated with pyloric atresia (JEB-PA with defects in α6β4 integrin (**E**), EB simplex associated with muscular dystrophy (EBS-MD with defects in plectin) (**F**), NLJEBBP180 with defects in BP180 (**G**), and severe recessive dystrophic EB (SRDEB with collagen VII defects (**H**). In control and SRDEB patients' skin, laminin-5 γ2 chains were normally expressed (**I** and **L**, respectively) using the γ2 chain monoclonal antibody GB3. Laminin-5 expression was severely reduced and absent in both the NLJEB and HJEB cases (**J,K**), respectively, harboring severe defects in laminin 5. Bar = 50 μm.

Figure 5 The majority of laminin 5 and laminin 10/11 chains are restricted to the lamina densa beneath HDs, whereas collagen IV is expressed continuously along the basal lamina. Postembedding immunoelectron microscopy with anti-α5 chain (laminin 10) (**A–D**) and double labeling with anti-α3 chain (laminin 5) (**E**) antibodies in control skin reveals a similar labeling pattern for these laminins. Collagen IV (M3F7), however, is not restricted to beneath HDs but is continuous along the basal lamina (**F**). Double labeling with laminin 5 polyclonal antiserum (15 nm gold particles) and laminin 10/11 (with smaller 5 nm gold particles) shows that the majority of labeling colocalizes beneath HDs at the border between the lamina lucida and lamina densa (**E**). The majority (84%) of laminin α5 chain labeling (see Table 2 and **A–D**) was restricted to areas immediately beneath the HDs, over the LD border (**A–D**, arrows) whereas only 61% of collagen IV was restricted to beneath HDs (**F**). HD plaques (solid arrows) are shown within the keratinocyte cytoplasm (white cross) and the lamina lucida highlighted by asterisks. Bar = 0.2 μm.

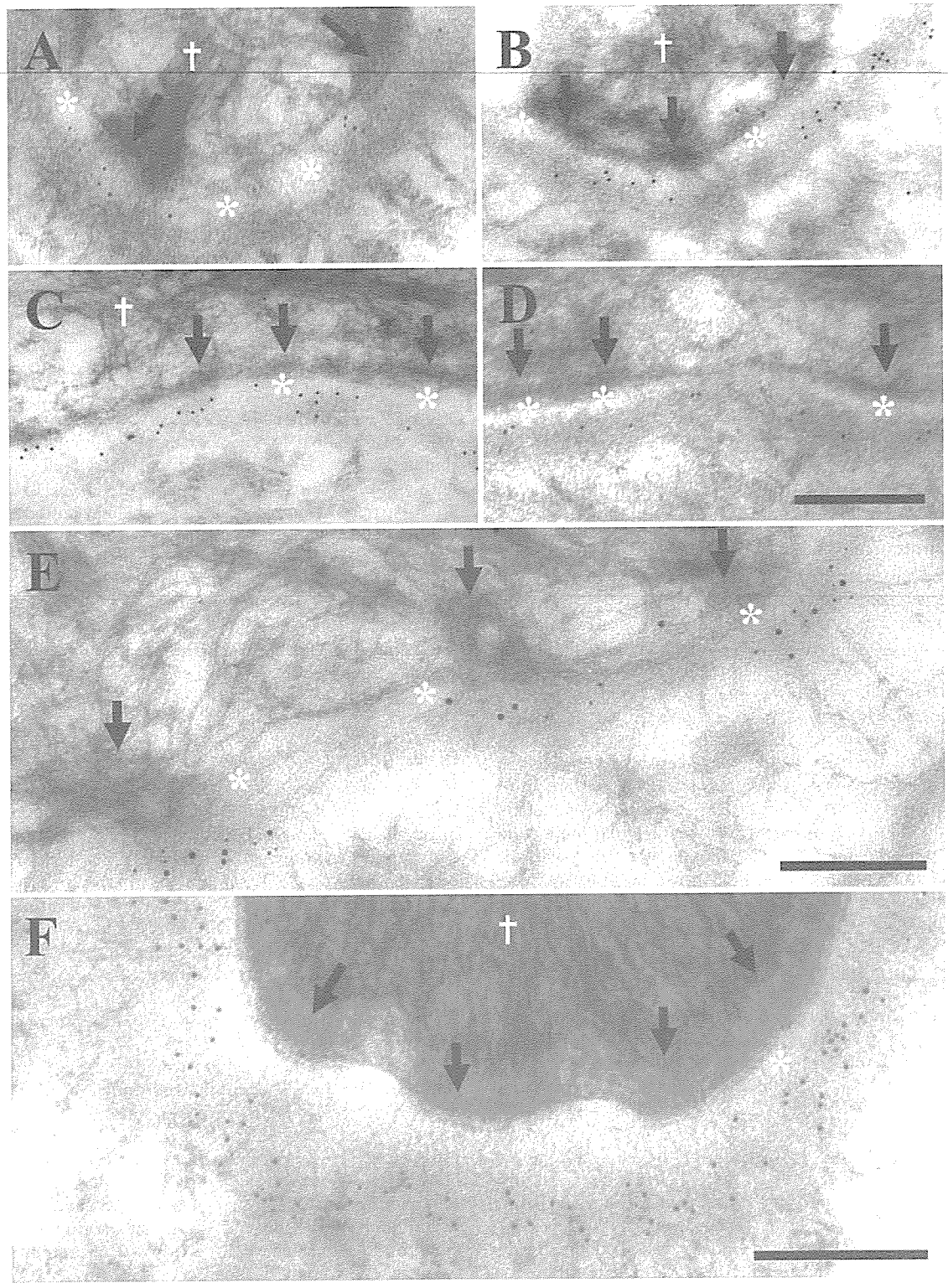

The Journal of Histochemistry & Cytochemistry

suggested that this effect might be due to antigen degradation in vivo in the split areas. The presence of α5 and β2 chains in intact EB skin, however, confirms that these chains are capable of being independently synthesized and assembled even in the total absence or in the presence of defective laminin 5. All other EB cases also showed normal staining for other laminins including junctional EB associated with pyloric atresia (JEB-PA) (with defects in α6β4 integrin, Figure 4E), EB simplex associated with muscular dystrophy (EBS-MD) (with defects in plectin, Figure 4F), non-lethal junctional (NLJEB) (with defects in BP180, Figure 4G), and severe recessive dystrophic epidermolysis bullosa (SRDEB) (Figure 4H). In control and SRDEB patients' skin there was normal staining for laminin 5 (γ2 chain using the antibody GB3, see Figure 4L). This was in contrast to laminin-5 chain staining that was severely reduced or absent in both the NLJEB (Figure 4J) and HJEB cases (Figure 4K), harboring severe defects in laminin-5 expression.

Immunogold Electron Microscopy and Quantitative Analysis

Labeling of control interfollicular epidermal sections showed that the majority of laminin-10 α5 chains (Figures 5A–5D; Table 2), β1, γ1, and 11 chain (β2 chain, data not shown) were restricted to under the cytoplasmic HD outer plaques. This was in contrast to collagen IV, which was not as restricted to beneath epidermal HDs plaques (see Figure 5F, 61% collagen IV vs 82% laminin 5). The difference between all laminin and collagen values was statistically significant using the one-way ANOVA ($p<0.001$) and Student's t-test ($p<0.000$). All four α5, β1, β2, and γ1 chain antibodies and antiserum showed a remarkable similarity in the percentage of labeling associated with the HD attachment plaque and anchoring filament complex beneath HDs, ranging between 84% and 92% (see Table 2). Furthermore, these values reflect an almost identical (HD restricted) expression pattern to the previously reported values for laminin-5 subunits (Masunaga et al. 1996; McMillan et al. 2003b) (part of these findings are also included in Table 2). Our data are very similar to those of laminin 5 (α3 chain) that on average demonstrated 82% of labeling restricted to beneath HDs (see Table 2) at a distance ranging from 35 to 45 nm below the plasma membrane at the LL–LD junction (Masunaga et al. 1996; McMillan et al. 2003b). The precise distance of the 4C7 epitope on the C-terminal portion of the α5 chain was 53.07 nm (±6.69 SD) from the plasma membrane (arrows, Figures 5A–5D). This is 18 nm lower than the G1 domain of the laminin-5 α3 chain described previously (see Figure 1) (McMillan et al. 2003b). The difference between these two α chain mean values was statistically significant using the one-way ANOVA ($p>0.01$) and Student's t-test ($p=0.009$). However, visual examination of the distribution of these two antigens revealed overlapping values ~30–40 nm beneath the plasma membrane, the only difference being that the α5 chain showed a wider range of labeling that extended deeper in the LD compared with the α3 chain. The remaining three β1-, β2-, and γ1-chain antibodies recognized, as yet unidentified, epitopes on specific laminin chains and were therefore not included in the plasma membrane distance measurements. However, all three antibodies showed upper LD labeling (not shown), the majority of which were restricted to beneath HDs similar to the α5 chain. The three β1-, β2-, and γ1-chain antibodies were excluded from the distance measurements but were scored for their localization either beneath visible HD attachment plaques (as defined by McMillan and Eady 1996) or within inter-HD areas.

Double labeling for the α5 chain of laminins 10/11 (highlighted by 5-nm small gold particles) and whole anti-laminin 5 antiserum (shown by the larger 15-nm gold particles) shows a similar labeling pattern in the LD beneath electron densities presumed to be HDs (Figure 5E). HD plaques are visible within the keratinocyte cytoplasm (white cross) and the dermal–epidermal junction is separated by the LL (Figure 5E, asterisks). Together our data suggest that the α5 chains (including β1, β2, and γ1 chains, see Table 2) show a restricted expression pattern beneath HDs, similar to laminin 5 but unlike collagen IV.

Discussion

We have demonstrated that the α5, β1, and γ1 chains show a similar localization to laminin 5 in the human interfollicular epidermal basement membrane. These data support the presence of multiple laminin isoforms beneath HDs in the basement membrane at several different epidermal sites. A very different localization of collagen IV within the LD but not restricted to beneath HDs was observed. These data suggest a complex network of interactions between different basement membrane components beneath the epidermis (Ghohestani et al. 2001; McMillan et al. 2003a; Miner and Yurchenco 2004).

In addition we have demonstrated that the expression of the α5 and β2 chains is independent of laminin 5, as demonstrated by residual staining in HJEB patients' skin. The reduction in α5 and β2 chain expression in HJEB was only observed over separated, blistered areas of skin, suggesting that this effect is due to separation-induced antigen degradation in vivo. This was supported by reduced collagen IV staining in split areas of EB skin. This was confirmed after reduced collagen IV staining was observed within separated areas of HJEB skin samples (data not shown). Our

results also suggest that the presence of other laminins cannot fully compensate for defects in laminin-5-deficient HJEB skin (McMillan et al. 1997,1998). The α5 and β2 chains were also normally expressed in all other EB samples harboring defects in plectin, collagen XVII (bullous pemphigoid antigen 2), the α6β4 integrin, and collagen VII.

In previous reports (Aumailley and Rousselle 1999), the laminin β2 chain was not expressed in the epidermal basement membrane of neonatal foreskin. However, we showed weak, variable β2 chain expression (in thigh and arm skin) and absences in other body sites (scalp skin). We conclude that the lack of β2 staining may be due to several factors: antigen masking, a low-level expression, or site- or age-specific variations in human laminin β2 chain expression that may include posttranslational protein processing seen in other laminin isoforms (Miner et al. 1997).

Laminin 5, together with several HD-associated antigens, is expressed in a specific pattern around late anagen hair follicles that excludes staining around the dermal papilla area (Akiyama et al. 1995; Nutbrown and Randall 1995). Laminin-10 chains also show this similar expression pattern in late anagen hair follicles. Unlike laminin-5 and laminin-10 chains, we failed to observe any β2 chain expression (laminins 7/11) in any part of the adult hair follicle; however, this may be due to a low level of antigen expression or masking of the β2 chain epitope. The significance of these findings may be related to the specific growth phases of the lower non-permanent portion of the hair follicle.

In the laminin α5 chain knockout mouse, an unusual disruption in hair follicle morphogenesis was demonstrated (Li, et al., 2003). Li et al. (2003) reported that, in control mice, laminin 10 was present in murine elongating hair germs when other laminins were down-regulated, suggesting a specific role for this laminin in hair follicle development and follicular keratinocyte migration. Mouse skin lacking laminin 10 also contained fewer hair germs and follicles compared with control mice, and after transplantation experiments this skin showed a failure of hair germ elongation and defective basement membrane assembly. Intriguingly, treatment of these mice with purified exogenous laminin 10 corrected these defects and restored hair follicle development. Given that human hair follicles are slow cycling and the majority remains in the late anagen phase and shows different growth characteristics to murine follicles, our failure to demonstrate such growth phase-specific differences in the expression of laminin 10 during the hair cycle stages is not surprising.

The presence of multiple laminin isoforms beneath HDs suggests the hypothesis that there are laminin subunits possibly with overlapping functions that form focal clusters of laminin molecules. This was in contrast to collagen IV, which was not restricted to HDs and localized to the LD region. Ultrastructural data show that the α3 chain (laminin 5) is closer to the plasma membrane than the α5 chain (with only an 18-nm difference, see Table 2). This might suggest that the α5 chain is more closely associated with a LD component such as collagen IV. However, given the size of both laminin chains of ~80–100 nm (as determined by rotary shadowing experiments), our data suggest a significant overlap occurs between α3 and α5 chains (Marinkovich et al. 1992; Vailly et al. 1994). Further studies using a larger battery of antibodies are required to determine the orientation of these laminin components.

Together these data show for the first time that laminin 10/11 chains are restricted to beneath HDs similar to laminin 5 but distinct from collagen IV. Our data suggest a specific localization of multiple laminin isoforms in the epidermal basement membrane beneath HDs and support the hypothesis that several laminins in close association may promote stable cell attachment among different basement membrane molecules.

Acknowledgments

This work was supported by a grant-in-aid of Scientific Research A (13357008, HS) and Health and Labor Sciences Research Grants (Research into Specific Diseases) H13-Saisei-02 and H17-Saisei 12, by a grant from the Japanese Society for the Promotion of Science (JSPS) grant #00345 to J.R.M., and by a grant-in-aid for JSPS fellows' research expenses (#00345). This work was also supported by a grant from the Japanese Health Science Foundation for Research Residents, for class "A" researchers (JRM).

We gratefully acknowledge the technical support of Ms. M. Sato and Ms. K. Sakai in this study. We also thank Dr. T. Masunaga for kindly providing the data from the γ2 chain study (Masunaga et al. 1996) and Dr. M.P. Marinkovich for his kind gift of his polyclonal laminin 5 antibody. Hybridoma supernatants D18 and 2E8 (produced by Drs. J. Sanes and E. Engvall) and M3F7 (from Dr. H. Furthmeyer) were obtained from the Developmental Studies Hybridoma Bank, developed under the auspices of the National Institute of Child Health and Human Development (NICHD) and maintained by the University of Iowa, Department of Biological Sciences, Iowa City, Iowa.

Literature Cited

Akiyama M, Dale BA, Sun TT, Holbrook KA (1995) Characterization of hair follicle bulge in human fetal skin: the human fetal bulge is a pool of undifferentiated keratinocytes. J Invest Dermatol 105: 844–850

Aumailley M, Rousselle P (1999) Laminins of the dermo-epidermal junction. Matrix Biol 18:19–28

Engvall E, Davis GE, Dickerson K, Ruoslahti E, Varon S, Manthorpe M (1986) Mapping of domains in human laminin using monoclonal antibodies: localization of the neurite-promoting site. J Cell Biol 103:2457–2465

Engvall E, Earwicker D, Haaparanta T, Ruoslahti E, Sanes JR (1990) Distribution and isolation of four laminin variants; tissue restricted distribution of heterotrimers assembled from five different subunits. Cell Regul 1:731–740

Foellmer HG, Madri JA, Furthmayr H (1983) Methods in laboratory investigation. Monoclonal antibodies to type IV collagen: probes

for the study of structure and function of basement membranes. Lab Invest 48:639–649
Geuijen CA, Sonnenberg A (2002) Dynamics of the α6β4 integrin in keratinocytes. Mol Biol Cell 13:3845–3858
Ghohestani RF, Li K, Rousselle P, Uitto J (2001) Molecular organization of the cutaneous basement membrane zone. Clin Dermatol 19:551–562
Gu J, Sumida Y, Sanzen N, Sekiguchi K (2001) Laminin-10/11 and fibronectin differentially regulate integrin-dependent Rho and Rac activation via p130(Cas)-CrkII-DOCK180 pathway. J Biol Chem 276:27090–27097
Hunter DD, Shah V, Merlie JP, Sanes JR (1989) A laminin-like adhesive protein concentrated in the synaptic cleft of the neuromuscular junction. Nature 338:229–234
Kennedy AR, Heagerty AH, Ortonne JP, Hsi BL, Yeh CJ, Eady RA (1985) Abnormal binding of an anti-amnion antibody to epidermal basement membrane provides a novel diagnostic probe for junctional epidermolysis bullosa. Br J Dermatol 113:651–659
Kikkawa Y, Sanzen N, Fujiwara H, Sonnenberg A, Sekiguchi K (2000) Integrin binding specificity of laminin-10/11: laminin-10/11 are recognized by α3β1, α6β1 and α6β4 integrins. J Cell Sci 113:869–876
Kikkawa Y, Sanzen N, Sekiguchi K (1998) Isolation and characterization of laminin-10/11 secreted by human lung carcinoma cells. Laminin-10/11 mediates cell adhesion through integrin α3β1. J Biol Chem 273:15854–15859
Li J, Tzu J, Chen Y, Zhang YP, Nguyen NT, Gao J, Bradley M, et al. (2003) Laminin-10 is crucial for hair morphogenesis. EMBO J 22: 2400–2410
Makino M, Okazaki I, Kasai S, Nishi N, Bougaeva M, Weeks BS, Otaka A, et al. (2002) Identification of cell binding sites in the laminin α5-chain G domain. Exp Cell Res 277:95–106
Marinkovich MP, Lunstrum GP, Burgeson RE (1992) The anchoring filament protein kalinin is synthesized and secreted as a high molecular weight precursor. J Biol Chem 267:17900–17906
Masunaga T, Shimizu H, Ishiko A, Tomita Y, Aberdam D, Ortonne JP, Nishikawa T (1996) Localization of laminin-5 in the epidermal basement membrane. J Histochem Cytochem 44:1223–1230
McMillan JR, Akiyama M, Shimizu H (2003a) Epidermal basement membrane zone components: ultrastructural distribution and molecular interactions. J Dermatol Sci 31:169–177
McMillan JR, Akiyama M, Shimizu H (2003b) Ultrastructural orientation of laminin 5 in the epidermal basement membrane: an updated model for basement membrane organization. J Histochem Cytochem 51:1299–1306
McMillan JR, Eady RA (1996) Hemidesmosome ontogeny in digit skin of the human fetus. Arch Dermatol Res 288:91–97
McMillan JR, McGrath JA, Pulkkinen L, Kon A, Burgeson RE, Ortonne J-P, Meneguzzi G, et al. (1997) Immunohistochemical analysis of skin in junctional epidermolysis bullosa using laminin 5 chain specific antibodies is of limited value in predicting the underlying gene mutation. Br J Dermatol 136:817–822
McMillan JR, McGrath JA, Tidman MJ, Eady RA (1998) Hemidesmosomes show abnormal association with the keratin filament network in junctional forms of epidermolysis bullosa. J Invest Dermatol 110:132–137
Mercurio AM, Rabinovitz I, Shaw LM (2001) The α6β4 integrin and epithelial cell migration. Curr Opin Cell Biol 13:541–545
Miner JH, Patton BL, Lentz SI, Gilbert DJ, Snider WD, Jenkins NA, Copeland NG, et al. (1997) The laminin α chains: expression, developmental transitions, and chromosomal locations of α1–5, identification of heterotrimeric laminins 8–11, and cloning of a novel α3 isoform. J Cell Biol 137:685–701
Miner JH, Yurchenco PD (2004) Laminin functions in tissue morphogenesis. Annu Rev Cell Dev Biol 20:255–284
Niessen CM, Hogervorst F, Jaspars LH, de Melker AA, Delwel GO, Hulsman EH, Kuikman I, et al. (1994) The α6β4 integrin is a receptor for both laminin and kalinin. Exp Cell Res 211:360–367
Nishiyama T, Amano S, Tsunenaga M, Kadoya K, Takeda A, Adachi E, Burgeson RE (2000) The importance of laminin 5 in the dermal-epidermal basement membrane. J Dermatol Sci 24(suppl 1): S51–59
Nutbrown M, Randall VA (1995) Differences between connective tissue-epithelial junctions in human skin and the anagen hair follicle. J Invest Dermatol 104:90–94
Pouliot N, Saunders NA, Kaur P (2002) Laminin 10/11: an alternative adhesive ligand for epidermal keratinocytes with a functional role in promoting proliferation and migration. Exp Dermatol 11: 387–397
Pulkkinen L, Smith FJ, Shimizu H, Murata S, Yaoita H, Hachisuka H, Nishikawa T, et al. (1996) Homozygous deletion mutations in the plectin gene (PLEC1) in patients with epidermolysis bullosa simplex associated with late-onset muscular dystrophy. Hum Mol Genet 5:1539–1546
Sanes JR, Engvall E, Butkowski R, Hunter DD (1990) Molecular heterogeneity of basal laminae: isoforms of laminin and collagen IV at the neuromuscular junction and elsewhere. J Cell Biol 111: 1685–1699
Shimizu H, McDonald JN, Gunner DB, Black MM, Bhogal B, Leigh IM, Whitehead PC, et al. (1990) Epidermolysis bullosa acquisita antigen and the carboxy terminus of type VII collagen have a common immunolocalization to anchoring fibrils and lamina densa of basement membrane. Br J Dermatol 122:577–585
Shimizu H, McDonald JN, Kennedy AR, Eady RAJ (1989) Demonstration of intra- and extra-cellular localization of bullous pemphigoid antigen using cryofixation and freeze substitution for postembedding immuno-electron microscopy. Arch Dermatol Res 281:443–448
Takizawa Y, Pulkkinen L, Shimizu H, Lin L, Hagiwara S, Nishikawa T, Uitto J (1998a) Maternal uniparental meroisodisomy in the LAMB3 region of chromosome 1 results in lethal junctional epidermolysis bullosa. J Invest Dermatol 110:828–831
Takizawa Y, Shimizu H, Pulkkinen L, Hiraoka Y, McGrath JA, Suzumori K, Aiso S, et al. (1998b) Novel mutations in the LAMB3 gene shared by two Japanese unrelated families with Herlitz junctional epidermolysis bullosa, and their application for prenatal testing. J Invest Dermatol 110:174–178
Takizawa Y, Shimizu H, Pulkkinen L, Nonaka S, Kubo T, Kado Y, Nishikawa T, et al. (1998c) Novel premature termination codon mutations in the laminin γ2-chain gene (LAMC2) in Herlitz junctional epidermolysis bullosa. J Invest Dermatol 111:1233–1234
Takizawa Y, Shimizu H, Pulkkinen L, Suzumori K, Kakinuma H, Uitto J, Nishikawa T (1998d) Combination of a novel frameshift mutation (1929delCA) and a recurrent nonsense mutation (W610X) of the LAMB3 gene in a Japanese patient with Herlitz junctional epidermolysis bullosa, and their application for prenatal testing. J Invest Dermatol 111:1239–1241
Tiger CF, Champliaud MF, Pedrosa-Domellof F, Thornell LE, Ekblom P, Gullberg D (1997) Presence of laminin α5 chain and lack of laminin α1 chain during human muscle development and in muscular dystrophies. J Biol Chem 272:28590–28595
Uitto J, Pulkkinen L (2001) Molecular genetics of heritable blistering disorders. Arch Dermatol 137:1458–1461
Vailly J, Verrando P, Champliaud MF, Gerecke D, Wagman DW, Baudoin C, Aberdam D, et al. (1994) The 100-kDa chain of nicein/kalinin is a laminin B2 chain variant. Eur J Biochem 219: 209–218
Yu H, Talts JF (2003) β1 Integrin and α-dystroglycan binding sites are localized to different laminin-G-domain-like (LG) modules within the laminin α5 chain G domain. Biochem J 371:289–299

The Journal of Histochemistry & Cytochemistry

Mono-letter mnemonics in dermatology

A mnemonic is a device or code that helps an individual to memorize key information about something. Many people are using mnemonics in teaching as they have been proven to be a successful learning aid.[1] Recently, we have reviewed the use of mnemonics in dermatologic disorders.[2]

Many websites and books compile lists of mnemonics; thus, there may be more than one mnemonic for a given disorder. It is left to the individual to select one that he or she prefers.

It is not uncommon for individuals to devise their own methods of remembering facts by constructing a word, song, picture, or incident.[2] Self-made mnemonics are often particularly effective, as the time and creative energy devoted to their development result in increased recall.[1]

We wish to point out in this brief communication that using a word or phrase for mnemonics may at times become outdated, similar to a new edition of a book which replaces a previous one. Mnemonics, too, must accommodate new information so that students can reap the maximum benefit from this useful learning aid. Problems can arise when new information is added, because the addition of a letter to the existing word or phrase will ultimately change the composition of a mnemonic that has been in vogue for some time. For instance, the five painful tumors of the skin have been grouped nicely into the word "Bengal" (*b*lue rubber bleb nevus, *e*ccrine spiradenoma, *n*eurilemmoma/neuroma, glomus tumor, *a*ngiolipoma/angioleiomyoma/angiosarcoma, and *l*eiomyoma), or the phrase "blend an egg", but now, with the potential addition of *c*utaneous endometriosis/calcinosis cutis and *o*steoma cutis, its use may be rendered obsolete. The new mnemonic for painful cutaneous nodules is BENGAL CO,[1] where "CO" refers to the first letter of the last two tumors mentioned. In addition, a word or phrase that may be of interest to individuals in some countries, and easily recalled by them, might not be of interest elsewhere or may be difficult for persons in other places to recall.

We wish to highlight that one good technique that can be used in framing mnemonics is a mono-letter. With this technique, it is possible to avoid the unnecessary inclusion of letters that change the meaning of the word, it can be used globally and internationally, and it is easily remembered because of its acceptability. This has been welcomed by other specialties.[3]

The letters may be employed in independent words or in words contained in a large statement. An example of the latter is the memorable description of Dowling–Degos disease by Wilson-Jones and Grice:[4] *d*emonstrating *d*usky *d*appled *d*isfigurements and *d*ark *d*ot *d*epressions, and *d*isclosing *d*igitate *d*owngrowths *d*elving *d*ermally.

Here, we list some of the "mono-letter" mnemonics that can be used as an aid in teaching dermatology: "a" in Addison's disease [asthenia, areola pigmentation, arterial hypotension, alimentary abnormality (anorexia, symptoms of acute abdomen), anxiety, axillary and pubic hair thinning]; "d" and "m" in pellagra [dementia, diarrhea, dermatitis, death, meats (mostly fats), molasses, meal (corn)]; "l" in a dermatopathology pattern with superficial and deep perivascular infiltrates with lymphocytes predominant [light eruption (polymorphus), lupus erythematosus, lymphocytic infiltrate of Jessner + deep figurate/gyrate erythema, Lyme disease, lues (syphilis) (+ plasma cells), lymphoma, leukemia, leprosy, indeterminate type (+ histiocytes)]; "p" in telogen effluvium (pregnancy, protein depletion, pills, propranolol, pyrexia, parturition, psychic stress); "p" in lichen planus (purple, polygonal, planar or flat, papules, pruritic, persistent, penile); "s" in superficial chronic glossitis [smoking, spirit (alcohol), spices, syphilis, sharp objects (trauma), sepsis (chronic debilitating diseases)].

Daifullah Al Aboud, MD
Khalid Al Aboud, MD
V. Ramesh, MD
Hafer Albaten and Makkah, Saudi Arabia and
New Delhi, India

References

1 Bouganim N, Barankin B, Freiman A. Mnemonics in dermatology. *Int J Dermatol* 2006; **45**: 81–82.
2 Al Aboud K, Al Hawsawi K, Ramesh V, *et al.* Mnemonics in dermatology; an appraisal. *Int J Dermatol* 2002; **41**: 594–595.
3 Evan RG. The four S's of Ewing's sarcoma. *Int J Radiat Oncol Biol Phys* 1991; **21**: 1671–1673.
4 Wilson-Jones E, Grice K. Reticulate pigmented anomaly of flexures (Dowling–Degos): a new genodermatosis? *Br J Dermatol* 1974; **91** (Suppl. 36): 6.

Aggressive squamous cell carcinoma developing in a giant epidermal cyst of the abdomen

Epidermal cysts (ECs) are common benign skin tumors. The development of malignant tumors within ECs is rare. We report a case of aggressive squamous cell carcinoma (SCC) developing in a giant EC of the abdomen.

A 48-year-old Japanese woman was referred to our clinic with a gradually enlarging, painful tumor on the right lower abdominal area, which had been incised and biopsied at the previous hospital 20 days earlier. The biopsy specimen demonstrated poorly differentiated atypical keratinocytes, suggesting the development of SCC. She had noticed the tumor for more than a decade; however, it had enlarged rapidly during the previous 6 months. Physical examination revealed a 7.6 × 4.1-cm cystic nodule on the right lower abdominal area (Fig. 1a,b). White keratinous material and pus were drained

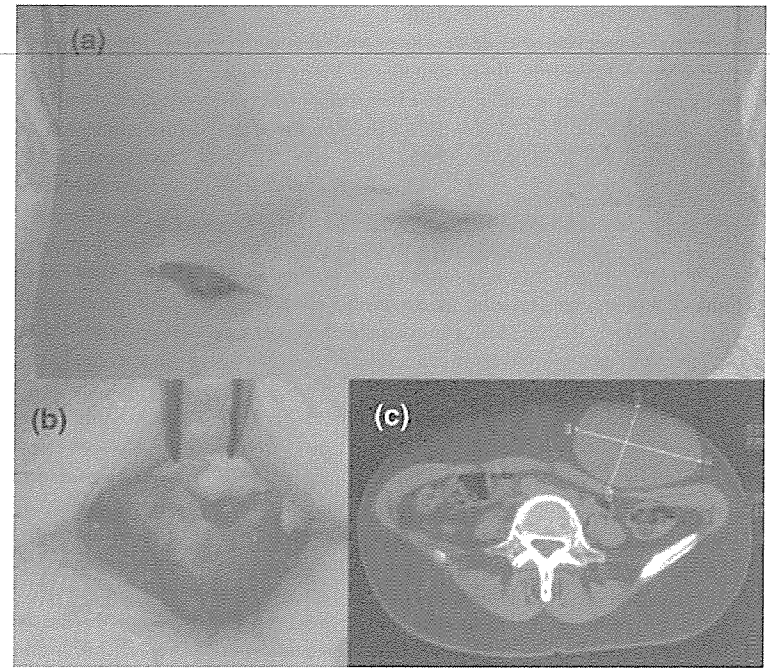

Figure 1 (a,b) Physical examination revealed a cystic nodule on the right lower abdominal area. (c) Computed tomography scan, performed at the previous hospital, showed a 9.3 cm × 6.6 cm cystic tumor. No invasion of the rectus abdominis muscle was suspected

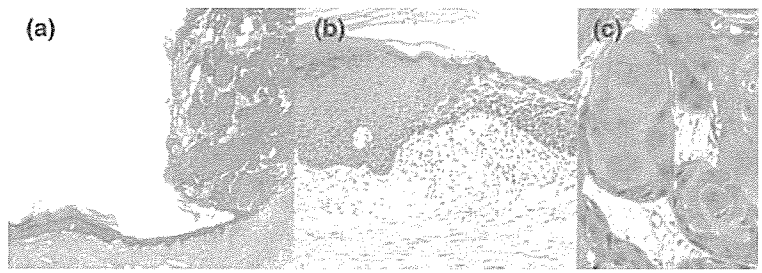

Figure 2 (a) Histologic observation of the nodule removed from the abdominal area revealed a tumor composed of normal cyst walls with a continuum to exophytic proliferation of atypical cells (hematoxylin and eosin stain, ×100). (b) Cyst wall composed of benign squamous epithelium with transition to squamous cell carcinoma (hematoxylin and eosin stain, ×200). (c) Atypical cells with distinct intercellular bridges and keratinized towards the center of the nest to form a cancer pearl (hematoxylin and eosin stain, ×400)

from the surgical scar. Computed tomography (CT) scan, performed at the previous hospital, showed a 9.2 × 6.6-cm huge cystic tumor, just above the abdominal fascia (Fig. 1c). For both diagnostic and therapeutic purposes, the tumor was excised with a 2-cm margin including the anterior layer of the rectus abdominis sheath. Microscopic examination of the surgical samples revealed exophytic proliferation of poorly differentiated squamous cells developing from the cyst wall (Fig. 2a), which was composed of benign squamous epithelium showing epidermal keratinization (Fig. 2b). In high-power view, poorly differentiated polygonal pleomorphic squamous cells with hyperchromatic nuclei were shown invading the dermis (Fig. 2c). Multiple atypical mitosis was also observed. Although the surgical margin was free of cancer cells, and the systemic CT scan and gallium scintigraphy demonstrated no metastasis at the time of surgical excision, the patient experienced cough and dyspnea 4 months after the excision. Chest CT and transbronchial lung biopsy revealed lung metastasis of SCC. Systemic chemotherapy with 1000 mg of 5-fluorouracil (5-FU) for 5 days and 100 mg of cisplatin for 1 day was initiated; however, the metastatic lesions spread rapidly, and the patient died as a result of respiratory failure 10 months after the operation. The subsequent autopsy confirmed multiple metastasis of SCC to the kidney, liver, mesentery, peritoneum, and skin.

SCCs arising from ECs are rare, and only 10 cases have been published in the English medical literature.[1–10] In these cases, ECs had been present for 2–132 months (mean, 34 months). The cyst size ranged from 1 to 10 cm in diameter (mean, 4.8 cm), and rapidly enlarged during the last 6 months in the majority of cases. Of these 10 cases, lymph node metastasis developed in only one. In our case, the size of the EC was large (10 cm in diameter), which may be related to the most aggressive clinical course reported so far. Another factor which may have affected the clinical outcome was that the lesion was incised for biopsy. Because of the incisional procedure, the boundary of the tumor may have become obscure, and the cancer cells may have been scattered to the surrounding tissue. In this case, both the large size and stimulation as a result of the incision may have led to the unfavorable clinical course.

Although the development of SCC within EC is relatively rare, the rapid enlargement of long-standing EC may be a sign of SCC development. In such cases, adequate and complete excision of the tumor is recommended to rule out the occurrence of SCC. Further systemic evaluation and careful follow-up of the patient are indicated because of the possibility of the rapid systemic metastasis, as observed in our case.

Ikue Nemoto, MD
Akihiko Shibaki, MD, PhD
Satoru Aoyagi, MD
Yukiko Tsuji-Abe, MD, PhD
Hiroshi Shimizu, MD, PhD
Sapporo, Japan

References

1 Devies MS, Nicholson AG, Southern S, *et al.* Squamous cell carcinoma arising in a traumatically induced epidermal cyst. *Injury* 1994; 25: 116–117.
2 Shah LK, Rane SS, Holla VV. A case of squamous cell carcinoma arising in an epidermal cyst. *Indian J Pathol Microbiol* 1989; 32: 138–140.
3 Arianayagam S, Jayalakshmi P. Malignant epidermal cyst: a case report. *Malaysian J Pathol* 1987; 9: 89–91.
4 Yaffe HS. Squamous cell carcinoma arising in an epidermal cyst. *Arch Dermatol* 1982; 118: 961.
5 Miller JM. Squamous cell carcinoma arising in an epidermal cyst. *Arch Dermatol* 1981; 117: 683.
6 Bauer BS, Lewis VL. Carcinoma arising in sebaceous and epidermoid cysts. *Ann Plast Surg* 1980; 5: 222–224.
7 Davidson TM, Bone RC, Kiessling PJ. Epidermoid carcinoma arising from within an epidermoid inclusion cyst. *Ann Otol Rhinol Laryngol* 1976; 85: 417–418.
8 Lopez-Rios F, Rodriguez-Peralto JL, Castano E, *et al.* Squamous cell carcinoma arising in a cutaneous epidermal cyst: case report and literature review. *Am J Dermatopathol* 1999; 21: 174–177.
9 Cameron DS, Raymond L. Squamous cell carcinoma arising in an epidermal inclusion cyst: case report. *Otolaryngol Head Neck Surg* 2003; 129: 141–143.
10 Malone JC, Sonneir GB, Huges AP, *et al.* Poorly differentiated squamous cell carcinoma arising within an epidermoid cyst. *Int J Dermatol* 1999; 38: 556–558.

Itraconazole in the treatment of cutaneous leishmaniasis

Dear Sir,

We read with great interest the paper by Dr Consigli *et al.*[1] reporting on the successful treatment of two cases of cutaneous leishmaniasis (CL) with itraconazole.[1]

There are other reports which support the results of Dr Consigli *et al.* with oral administration of itraconazole in the treatment of CL, which were not referenced in the aforementioned article, but when considering the hierarchy of evidence for therapeutic studies it is generally accepted that randomized, controlled, clinical trials (RCTs) provide more reliable evidence than case reports.[2–4] It is for this reason that the emphasis of this letter is on the RCTs concerning efficacy of oral itraconazole in the treatment of CL.

Dr Consigli *et al.* referred to four RCTs to support their results, including two studies from India, one article from Kuwait and one from Iran.[5–8]

We wish to mention some points regarding the RCTs that Dr Consigli *et al.* used to support their results. Dr Consigli *et al.* referenced a paper by Momeni *et al.*[8] to support the efficacy of itraconazole in the treatment of CL. It should be considered that Momeni *et al.* mentioned at the conclusion of their paper that "the low response rate in patients receiving itraconazole indicates that itraconazole cannot be used as the single agent in the treatment of patients with CL caused by *L.* major".[8]

Dogra *et al.*, in two small sample RCTs of 20 and 24 patients with CL, compared the results of treatment with oral itraconazole with no treatment, or placebo, for 6 weeks in an endemic area for *L. tropica* and concluded that oral itraconzole had promising antileishmanial potential.[5,6] In another small size RCT in Kuwait, involving a total of 24 cases with CL, the authors concluded that itraconazole appeared to be a suitable antileishmanial drug with minor side-effects in comparison with those reported with pentavalent anitimoniate.[7]

We also wish to refer to a more recently published double-blind, placebo-controlled RCT on 200 patients in an endemic area for CL, owing to *L. major*, in which the efficacy of an 8-week course of oral itraconazole at a dose of 200 mg/day was not significantly different from the placebo: 59% vs. 53%, respectively.[9]

All the above-mentioned reports evaluated treatment with itraconazole in Old World CL. Although we could not find any appropriately designed RCTs concerning itraconazole in

Induction of Therapeutically Relevant Cytotoxic T Lymphocytes in Humans by Percutaneous Peptide Immunization

Hiroaki Yagi,[1] Hideo Hashizume,[1] Takahiro Horibe,[1] Yasushi Yoshinari,[1] Maki Hata,[1] Akihiro Ohshima,[1] Taisuke Ito,[1] Masahiro Takigawa,[1] Akihiko Shibaki,[2] Hiroshi Shimizu,[2] and Naohiro Seo[1]

[1]Department of Dermatology, Hamamatsu University School of Medicine, Hamamatsu, Japan and [2]Department of Dermatology, Hokkaido University Graduate School of Medicine, Sapporo, Japan

Abstract

Percutaneous peptide immunization (PPI) is a simple and noninvasive immunization approach to induce potent CTL responses by peptide delivery via skin with the stratum corneum removed. After such a barrier disruption in human skin, epidermal Langerhans cells, although functionally matured through the up-regulation of HLA expression and costimulatory molecules, were found to emigrate with a reduced number of dendrites. $CD8^+$ populations binding to MHC-peptide tetramers/pentamers and producing IFN-γ appeared in the blood after PPI with HLA class I–restricted antigenic peptides. PPI with melanoma-associated peptides reduced the lesion size and suppressed further development of tumors in four of seven patients with advanced melanoma. These beneficial effects were accompanied by the generation of circulating CTLs with *in vitro* cytolytic activity and extensive infiltration of tetramer/pentamer-binding cells into regressing lesions. PPI elicited neither local nor systemic toxicity or autoimmunity, except for vitiligo, in patients with melanoma. Therefore, PPI represents a novel therapeutic intervention for cancer in the clinical setting. (Cancer Res 2006; 66(20): 10136-44)

Introduction

Dendritic cell (DC)-based immunotherapy for cancer and infection is feasible, safe, and effective in some cancer patients when appropriately matured and activated DCs are administered (1–11). However, because of the lack of standardization in methods for *in vitro* generation of DCs and protocols to administer these vectors, comparison of clinical efficacy among DC immunotherapies, and thus, designing large clinical trials seems to be difficult (12). More critically, the intricate processes involved are costly and time-consuming, constituting an obstacle to clinical application of DC-based strategies. Targeting DCs should be ideally done *in vivo* (12, 13).

Epidermal Langerhans cells (LC), immature DCs residing in the outermost layer of the skin, become potent antigen-presenting cells (APC) after appropriate stimulation (14, 15). Because of their unique anatomic localization and immune functions, LCs are very attractive vectors for vaccine delivery (14, 16–19). Percutaneous peptide immunization (PPI) represents a novel immunotherapy using LCs as vectors for delivering all classes of peptide to the immune system. Removal of the stratum corneum (SC), the most superficial layer of the epidermis, by physical means, is essential in this simple and noninvasive method (20). The barrier removal process not only enhances the permeability of antigenic peptides applied to the skin but also matures LCs for antigen presentation (21). Following migration from barrier-disrupted skin to lymphoid organs, LCs bearing peptides induce potent CTL responses. Experiments in murine tumor models have shown that this simple and safe procedure is highly effective for prophylaxis and therapy of infection and tumors (19, 20, 22). The present study was designed to validate PPI as a clinical intervention for the management of malignancies in humans.

Materials and Methods

Human Subjects

A total of eight healthy males, with ages ranging from 24 to 56 years, and eight patients with stage III/IV melanoma (P1-P8; Table 1) were enrolled in the present study. Three healthy males, designated N1 (age, 35 years), N2 (40 years), and N3 (30 years), all having HLA-A*0201, underwent PPI with HIV gag peptides. Another six healthy subjects, with ages ranging from 24 to 56 years, participated in clinical and immunohistochemical studies following the removal of SC but did not receive PPI. Patients with melanoma received PPI with melanoma-associated antigenic peptides. Eligible criteria for PPI in the patients were: biopsy-proven American Joint Committee on Cancer stage III/IV melanoma; age, ≥20 years; Eastern Cooperative Oncology Group performance status, ≤1 on entry of PPI; HLA-A*0201 and/or HLA-A*2402 phenotype; normal blood CD4 and CD8 T cell numbers by flow cytometry; and normal quantitative immunoglobulin levels. Exclusion criteria were: prior chemotherapy or application of biologicals ≤4 weeks before trial entry, untreated lesions in the central nervous system, bulky hepatic metastatic lesions, pregnancy, and concurrent corticosteroid/immunosuppressive therapy. Patients with generalized inflammatory skin disease, autoimmune disease, or active infections, including viral hepatitis, were also excluded. P1 to P4, P7, and P8 developed metastatic lesions despite initial treatment involving wide local excision and therapeutic lymph node dissection followed by postoperative combination adjuvant therapy (23). P6 developed primary esophageal melanoma. Due to resection of all the skin lesions and metastatic lymph nodes, P1 was free from measurable lesions on entry and served for evaluation of CTL induction only. In contrast, due to the presence of measurable lesions on entry, both CTL induction and early clinical outcome were assessed in P2 to P8.

In all subjects, routine blood examinations including a hemogram, and assessment of liver and renal function and autoantibodies showed no abnormalities on entry to PPI treatment. Serologic tests for HIV were negative, whereas serum hemagglutination inhibition titers for influenza A virus showed positive results. This study was approved by the institutional

Note: H. Yagi and H. Hashizume contributed equally to this work.

Requests for reprints: Hiroaki Yagi, Department of Dermatology, Hamamatsu University School of Medicine, 1-20-1 Handayama, Hamamatsu 431-3192, Japan. Phone: 81-53-435-2303; Fax: 81-53-435-2368; E-mail: hiroyagi@hama-med.ac.jp.

doi:10.1158/0008-5472.CAN-06-1029

review board. Informed consent was obtained from all participants according to the Declaration of Helsinki.

Synthetic Peptides and Reagents

Three custom-synthesized peptides including HIV gag (SLYNTVATL), influenza A matrix protein (MP; GILGFVFTL; American Peptide Company, Inc., Sunnyvale, CA), and modified Melan-A immunodominant cells (ELAGIGILTV; Peptide Institute, Inc., Osaka, Japan; ref. 24), were used as HLA-A*0201-restricted epitopes and four custom-synthesized peptides including MAGE-2 (EYLQLVFGI), MAGE-3 (IMPKAGLLI), gp-100 (VWKTWGQYW), and tyrosinase (AFLPWHRLF; Peptide Institute) were used as HLA-A*2402-restricted epitopes. Their purity was >95.0% as confirmed by high-pressure liquid chromatography. Phycoerythrin (PE)-labeled MHC tetramers specific for the HIV gag and Melan-A peptides were purchased from Beckman Coulter (Villepinte, France) and PE-labeled MHC-pentamers for MAGE-2, MAGE-3, and tyrosinase were custom-synthesized by ProImmune Limited (Littlemore, United Kingdom). The monoclonal antibodies (mAb) used in this study were anti-S-100 protein (DAKO, Glostrup, Denmark), anti-DC-LAMP/CD208 (Beckman Coulter), anti-Langerin/CD207 (Vector, Burlingame, CA), PE-labeled or PerCP-labeled anti-HLA-DR, FITC-labeled anti-CD4, PE-labeled or PerCP-labeled anti-CD8 and PerCP-labeled anti-CD45 (BD Biosciences, San Jose, CA), PE-labeled anti-CD1a, FITC-labeled anti-HLA-ABC (pan-HLA class I), anti-CD80, and anti-CD86 (PharMingen, San Diego, CA). RPMI 1640 complete was used for culture medium (20).

Epidermal Barrier Disruption

To remove SC, 5 × 5 cm square plastic plates were painted evenly with ~100 mg/plate of cyanoacrylate (Aron alpha A, Sankyo, Japan), tightly attached to the skin for 3 minutes and removed gently. This procedure was repeated thrice at one spot.

Transepidermal Water Loss Evaluation

Transepidermal water loss (TEWL) was measured using a Tewameter TM210 (Courage + Khazaka Electronic GmbH, Köln, Germany) as previously described (21).

PPI

Solutions of immunization peptides were made immediately before use. HLA-A*0201 subjects received 10 mg of HIV gag peptide in 10 mL of PBS or 16 mg of Melan-A peptide in 8 mL of 5% DMSO in PBS (5% DMSO). A cocktail of 5 mg each of MAGE-2, tyrosinase, and gp-100 peptides in 10 mL of PBS, and 4 mg of MAGE-3 peptide in 2 mL of 5% DMSO, were used for HLA-A*2402 subjects. These concentrations represented the saturation points of the peptides at room temperature. In P3 and P8, who had both HLA-A*0201 and HLA-A*2402, the MAGE-3 peptide solution contained 4 mg of Melan-A peptide. Twenty-four hours after the removal of SC, these peptide solutions were soaked up by gauze pads (each 5 × 5 cm) and applied to four barrier-disrupted areas (total area, 100 cm^2) of HLA-A*0201 subjects and to the six areas (total area, 150 cm^2) of both HLA-A*2402 subjects and individuals with both alleles. The pads were immediately covered with a film dressing and removed 24 hours later. PPI was repeated six times in normal volunteers and seven times in patients with melanoma at monthly intervals by placing the patches at different sites of the arms, thighs, abdomen, and back. Assessment of hemograms, and liver and renal functions was done 1 week following each PPI and at 1- to 3-month intervals thereafter.

Skin Specimens and Epidermal Cell Suspensions

Biopsy specimens were processed for routine histology and immunohistochemistry (25). The epidermal sheets were separated from the dermis in 0.02 mol/L of EDTA-PBS at 4°C for 18 hours and subjected to immunohistochemical staining. Epidermal suspensions were prepared from blister roofs by limited trypsinization (26).

Identification of LCs

Cells expressing S-100 protein in epidermal sections, and those positive for HLA-DR and CD1a in epidermal sheets and suspensions were identified as LCs (14, 27). Immunostained epidermal sheets were observed in a confocal laser scanning microscope (MRC-600; Bio-Rad, Hercules, CA; ref. 27). Epidermal cell suspensions were stained with a PE-labeled anti-CD1a mAb, a PerCP-labeled anti-HLA-DR mAb, and any one of an FITC-labeled anti-HLA-ABC mAb, an FITC-labeled anti-CD80 mAb, an FITC-labeled anti-CD83 mAb, an FITC-labeled anti-CD86 mAb, or FITC-labeled control antibodies and subjected to flow cytometry.

Flow Cytometry

Samples were run on a FACSCalibur flow cytometer (BD Biosciences) using CellQuest Software as described (28, 29). Three × 10^4 and 2 × 10^5 events were analyzed for epidermal samples and blood cells, respectively. For analysis of the epidermal samples, only size gates were used for counting the total number of HLA-ABC$^+$ epidermal cells. Gates for LCs were set as described in the legend for Fig. 1.

Measurement of Immune Responses

Peripheral blood mononuclear cells (PBMC) were purified before and 7 days after each PPI by standard Ficoll density centrifugation and subjected to flow cytometric analysis for cell surface staining and intracellular IFN-γ expression. Because binding to tetramers and pentamers and IFN-γ staining are highly reproducible with a variation of <5%, when the number of positive cells was +2 SD above the mean background staining, we defined this as the specific induction of antigen-specific CTLs.

Cell culture. PBMCs (5 × 10^6 cells/well in complete medium in 12-well tissue culture plates) were stimulated with immunization peptide (10 μg/mL), influenza A MP (10 μg/mL), or Con A (1 μg/mL; Sigma-Aldrich, St. Louis, MO) for 5 days and underwent either tetramer or pentamer staining and *in vitro* cytotoxic assay. Alternatively, cells cultured for 48 hours were subjected to intracellular IFN-γ production. Control cultures contained no stimulant. PBMCs from HLA-A*0201 or HLA-A*2402 subjects without PPI were cultured under identical conditions.

MHC tetramer and pentamer staining. Fresh or cultured PBMCs were stained with PE-labeled HLA-A*0201 tetramers or PE-labeled HLA-A*2402 pentamers and a gating kit (Beckman Coulter) according to the manufacturer's directions.

Intracellular IFN-γ analysis. GolgiStop (0.7 μL/mL, PharMingen) was added to cultures 8 hours before harvesting. Cells were reacted with a PerCP-conjugated anti-CD8 mAb, permeabilized in CytoFix/Cytoperm plus Perm/Wash buffers (PharMingen), and stained with an FITC-labeled anti-IFN-γ mAb (PharMingen). Control levels were determined with an appropriate isotype-matched antibody in each experiment.

***In vitro* peptide-dependent cytotoxic assay.** Only cultures containing >5% of tetramer-positive or pentamer-positive cells among CD8$^+$ cells following peptide stimulation were further expanded with rIL-2 (10 units/mL) for 3 days for effector cells. T2-A24 target cells (1 × 10^6 cells; T2 cell line transfected with HLA-A*2402 gene; ref. 30) incubated with immunizing peptide at 1 μg/mL for 1 hour were subjected to both HLA-A2-restricted and HLA-A24-restricted, calcein-AM release CTL assays (Dojindo Lab., Kumamoto, Japan). Briefly, T2-A24 cells were labeled with 5 μmol/L of calcein-AM in serum- and phenol red–free Iscove's modified Dulbecco's medium (IMDM; Invitrogen Co., Carlsbad, CA) at a concentration of 2 × 10^6 cells/mL for 40 minutes. Effector and target cells in 200 μL of IMDM supplemented with 10% FCS were distributed into U-bottomed 96-well microtiter plates at effector/target ratios of 2, 5, and 10. After incubation at 37°C for 3 hours, the concentration of calcein-AM in the medium was measured in a fluorescence analyzer (Synergy HT, Bio-Tek Inst., Inc., Winooski, VT). Maximal lysis was determined by adding lysis buffer to target cells and percentage-specific lysis were calculated as described previously (31).

Therapeutic PPI and Assessment of Early Clinical Outcome

Based on the kinetics of CTL generation in the blood, we instituted a treatment plan of PPI for patients with melanoma consisting of immunization with melanoma-associated peptide, seven times in total, done once a month. All baseline evaluations were done on entry. Tumor responses and side effects were assessed based on physical examination and laboratory investigation after completion of PPI. To assess tumor responses, the size of target lesions selected according to the Response Evaluation Criteria in Solid Tumors guidelines (32) was measured before and after PPI. Imaging-based evaluations were analyzed using NIH Image software for digital images. In P8, the dot densities in ^{99m}technetium

Table 1. Patient characteristics, disease status on entry and after PPI, and immunologic and clinical responses to PPI

Patient ID*	Age/gender	HLA-A		Stage/months after staging/previous therapy	Status/measurable disease on entry/number of target lesions	% $CD3^+$ $CD8+$ T cells in peripheral blood †	Number of peptide-specific T cells/10^4 $CD8^+$ cells in pre-PPI/post-PPI blood samples	
		02/01	24				Melan-A ‡	Tyrosinase ‡
P1	53/F	+	–	Stage IV/48/surgery, DAV-feron	CR/surgical removal of all skin and LN lesions/0	20.4	2/36	ND
P2	78/F	–	+	Stage III/7/surgery, DAV-feron	PD‖/surgical removal of all skin and LN lesions/0	19.8	ND	12/53
P3	77/M	+	+	Stage IV/20/surgery, DAV-feron	PD/mediastinal LN mass by CT and ^{67}Ga scintigraphy/1	16.8	2/94	11/61
P4	20/M	–	+	Stage IV/7/surgery, DAV-feron	PD/skin, lung and liver nodules by CT and MRI/10	27.2	ND	19/22
P5	68/F	–	+	Stage IV/5/surgery	PD/s.c. nodules by CE and CT/5	21.7	ND	15/14
P6	52/M	–	+	Stage III/2/none	PD/esophageal mass by CT and endoscopy/1	20.5	ND	6/105
P7	63/M	+	–	Stage IV/6/surgery, DAV-feron	PD‖/s.c. nodule by CE/1	24.2	1/118	ND
P8	77/M	+	+	Stage IV/5/surgery, DAV-feron	PD/multiple bone metastases by ^{99m}Tc bone scintigraphy/6	17.2	4/113	9/75

Abbreviations: CE, clinical examination; CR, free from melanoma for >4 weeks before entry; CT, computed tomography; DAV-feron, adjuvant therapy with i.v. dacarbazine, nimustine hydrochloride, and vincristine plus lesional injection of IFN-β; LN, lymph node; MRI, magnetic resonance imaging; PD, progression of measurable disease and/or new lesions; ND, not done.

*Patient ID, patient identification number.

† Percentages after lymphocyte gating by flow cytometry.

‡ Number of cells positive for MHC tetramers or pentamers/10^4 $CD8^+$ T cells in freshly isolated PBMCs.

§Number of intracellular IFN-γ-positive cells/10^4 $CD8^+$ T cells in PBMCs stimulated with gp-100 peptide (10 μg/mL) for 48 hours and subjected to an intracellular IFN-γ assay.

‖P2 and P7 developed new metastatic skin nodules at frequencies of one and three per 2 months, respectively, before entry.

¶In P4 and P5, the sums of the longest diameters for 10 and 5 lesions, respectively, were measured as the pre-PPI and post-PPI sums of the longest diameters.

**The dot densities in ^{99m}technetium hydroxymethylene diphosphonate bone scintigraphs of the metastatic lesions (indicated in Fig. 4) pre-PPI/post-PPI were 98.4/60.8 (#1), 128.6/59.8 (#2), 72.3/55.1 (#3), 84.3/71.3 (#4), 135.8/118.5 (#5), and 101.3/100.8 (#6). The serum 5-S-cysteinyldopa level reduced from 27 nmol/L pre-PPI to 4.2 nmol/L post-PPI (normal, <8.0 nmol/L).

hydroxymethylene diphosphonate bone scintigraphs were compared before and after PPI. The mean background density was calculated based on the density of three unaffected areas in a scintigraph. After the mean background densities before and after PPI were equalized, the lesional density was determined by analyzing the densities of square-framed areas representing bone metastasis.

Statistical Analysis

Student's t test was employed for comparisons, with $P < 0.05$ considered significant.

Results

Clinical observations after removal of sc. After removal of SC, faint and transient erythema developed in the treated sites which disappeared within 1 hour. Subjective symptoms such as pain or skin irritation during or after the manipulation were minimal or absent.

Kinetics of LCs in barrier-disrupted skin. Tissue histology revealed that 60% to 80% of the SC was removed in normal subjects ($n = 3$), on comparison of the thickness of SC before and immediately after barrier disruption, using adjacent skin as a control (Fig. 1*A*). TEWL values significantly increased from 8.10 ± 0.66 before manipulation to 16.83 ± 2.20 g/m^2/h after the removal of SC ($n = 3$, $P < 0.05$), indicating that considerable barrier disruption occurred with the method employed. Recovery was already evident at 48 hours and there were minimal or no inflammatory responses after 12, 24, and 48 hours as revealed by tissue histology. $S\text{-}100^+$ LCs showed larger cell bodies with fewer dendrites after the removal of SC compared with their

Table 1. Patient characteristics, disease status on entry and after PPI, and immunologic and clinical responses to PPI (Cont'd)

Number of peptide-specific T cells/10^4 $CD8^+$ cells in pre-PPI/post-PPI blood samples			Sums of the longest diameters of pre-PPI/post-PPI target lesions (cm)	Clinical outcome after PPI/side effects	Follow-up
MAGE-2[‡]	MAGE-3[‡]	gp-100[§]			
ND	ND	ND	0/0	No new lesions/generalized, progressive vitiligo	Disease-free for 19 months after PPI
6/68	9/106	6/30	0/0	No new lesions/none	Three new s.c. nodules (<5 mm in size) at 3 months after first round of PPI, which disappeared after the second round of PPI
8/42	14/212	4/23	3.2/0.9	Normal LN size/generalized, progressive vitiligo	Disease-free for 15 months after PPI
6/34	22/189	4/3	22/32[¶]	New metastatic lesions/none during PPI	Early death due to melanoma lesions
4/34	14/206	8/9	17/8[¶]	Decrease in size of target lesions/generalized, progressive vitiligo	New cutaneous and metastatic lesions developed despite continuous immunization for 13 months
8/93	8/204	12/243	4.0/5.5	Enlargement of a lesion/ generalized vitiligo	Death due to melanoma lesions at 4 months after PPI
ND	ND	ND	2/0	No new lesions/none	Two new s.c. nodules (<5 mm in size) at 5 months after first round of PPI, which disappeared after second round of PPI
18/41	16/94	5/75	Reduced intensities of the scintigraphy signals[**]	No new lesions/none	New lesion at 4 months after PPI despite unchanged densities of previous lesions

counterparts in intact skin. Both epidermis and dermis at 12 and 24 hours harbored S-100^+ cells, whereas most of them were located in the dermis at 48 hours. HLA-DR^+ cells were found to be larger and stained more brightly at 12 and 24 hours in epidermal sheets (Fig. 1*A, inset*) as compared with the intact skin case. At 48 hours, Langerin$^+$ cells were distributed in both epidermis and dermis, whereas DC-$LAMP^+$ cells were found mainly in the dermis. Enumeration of $CD1a^+$ cells in HLA-ABC^+ epidermal cell suspensions showed that essentially all LCs remained in the epidermis at 12 and 24 hours, and about half of this population migrated into the dermis at 48 hours (Fig. 1*B*). Enumeration of LCs in the epidermal sheets of three individuals showed that the mean number of HLA-DR^+ cells were 83% of the intact skin case at 24 hours and 39% of the cells remained in the epidermis at 48 hours. In accordance with these morphologic observations, the expression of HLA-ABC and HLA-DR (Fig. 1*C*) was up-regulated and the numbers of $CD80^+$, $CD83^+$, and $CD86^+$ (Fig. 1*D*) cells in LC populations were increased at 12 and 24 hours. The cells expressing CD86 remained increased in number even at 48 hours. Fully mature LCs are recognized by their strong surface expression of MHC class I/class II, CD80, CD86 costimulatory molecules, and CD83 maturation markers (33). Therefore, these findings indicated LC subpopulations to be activated *in situ*, then emigrating from the epidermis following disruption of the epidermal barrier by removal of SC.

Induction of antigenic peptide-specific CTLs by PPI. Based on the LC kinetics, we reasoned that optimal CTL priming might be induced by the application of antigenic peptides 24 hours after barrier disruption and subsequent exposure of the skin sites to the peptides for 24 hours. Normal subjects (N1, N2, and N3) received PPI with the HIV gag peptide. Six patients with stage IV melanoma (P1, P3, P4, P5, P7, and P8) and two patients with stage III melanoma (P2 and P6) underwent PPI with melanoma-associated antigenic peptides. Application of peptide at SC-removed sites was well tolerated, without local reactions such as irritation, redness and erosion, or systemic toxicity evidenced by rashes, fatigue, or fever. None of the study participants experienced lymphadenopathy thought to be related to PPI.

The appearance of CTLs was assessed periodically in the peripheral blood with reference to cells positive for tetramers and pentamers and intracellular IFN-γ^+ cells. Representative data of CTL induction in normal subjects and melanoma patients are shown in Figs. 2 and 3. Tetramer/pentamer-positive $CD8^+$ T cells were successfully detected in freshly obtained blood when assayed 7 days after the fourth immunization with HIV gag in cases N1 to N3, and after the fifth to sixth immunization with melanoma-associated peptides in patients P1 to P3 (Fig. 2*A-C*). The frequencies of binding cells were maintained in N1 and N2, whereas frequencies were increased in N3, P1, P2, and P3 following repeated immunization. Such *in vivo* expansion of CTL in normal individuals and patients with melanoma was antigen-specific because tetramer-binding responses were apparently enhanced in cultures stimulated with immunizing peptide but not with nonimmunizing peptide (Fig. 2*D*). The generation of HLA-A*0201-restricted CTLs was also detected with Melan A-specific tetramers in P7 and P8. After completion of therapeutic PPI, P2, P3, P6, P7, and P8 developed $CD8^+$ T cells reactive with pentamers for tyrosinase, MAGE-2, and MAGE-3, whereas only MAGE-2-specific

and MAGE-3-specific binding occurred in P4 and P5 (Table 1). Application of the HIV gag peptide to intact skin for 24 hours done once a month for five times did not induce CTL responses in N1 and N2. These data clearly indicate that repeated immunization induces and maintains antigenic peptide-specific CTLs.

Antigenic peptide-specific production of intracellular IFN-γ. Stimulation with Con A and Melan-A peptide induced significant numbers of intracellular IFN-γ^+CD8^+ T cells in patients undergoing PPI (Fig. 3*A*). PPI induced $CD8^+$ T cells with intracellular IFN-γ after the fifth immunization with the HIV gag in N1 to N3, and after the sixth and fourth immunization with Melan-A in P1 and P3, respectively (Fig. 3*B*). In addition, $CD8^+$ T cells positive for intracellular IFN-γ were expanded after stimulation *in vitro* with influenza A MP in HLA-A*0201-positive participants who were revealed to have functional antibodies for influenza A viruses by serologic studies. These observations not only indicated the presence of functional CTLs in the peripheral blood but also confirmed the feasibility of the present assay for detecting IFN-γ-producing cells. Four of six HLA-A*2402-positive melanoma patients (P2, P3, P6, and P8) developed gp-100-specific T cells positive for intracellular IFN-γ at completion of therapeutic PPI (Table 1). Therefore, we concluded that repeated immunization in PPI induces and maintains immunologically active, peptide-specific CTLs.

***In vitro* cytolytic function of PPI-induced CTLs.** In cytotoxic assays at completion of PPI, PBMCs from P2, P3, and P5 exerted a marked antigen-specific killing activity against HLA-A*2402 peptide-pulsed T2-A24 cells. Figure 3*C* shows the results of representative experiments with tyrosinase in P2. Effector cell populations contained 8.2%, 7.3%, and 6.7% peptide-matched pentamer-positive cells among $CD8^+$ cells in P2, P3, and P5, respectively. Optimal killing activity was observed with tyrosinase in P2, MAGE-2 in P3 (99.7 ± 5.9%, $P < 0.01$ compared with control; 56.2 ± 2.5%), and MAGE-3 in P5 (80.6 ± 3.4%, $P < 0.01$ compared with control; 54.6 ± 0.9%) at an effector-to-target ratio of 10. P1 and P3 also showed killing activity against HLA-A*0201-restricted target cells pulsed with Melan-A peptide (data not shown). The cytolytic activity was always detected in cultures which successfully proliferated on stimulation with immunizing peptide. CTLs from P4 could not be expanded to the level necessary for killing assays. Therefore, the therapeutic efficacy of PPI seemed to be correlated with *in vitro* effective propagation of peptide-specific CTLs with apparent cytolytic function.

Clinical efficacy of PPI for melanoma treatment. A critical issue is the therapeutic potency of PPI-induced CTLs. Therefore, the tumor response associated with the first round of therapeutic PPI was evaluated in P3 to P8 who had measurable lesions (Table 1). In P3, an enlarged mediastinal lymph node due to metastasis of melanoma cells decreased in size, from the longest diameter of 3.2 cm before PPI, to 0.9 cm at completion of PPI (Fig. 4*A*). P5 showed a >50% reduction in the sums of the longest

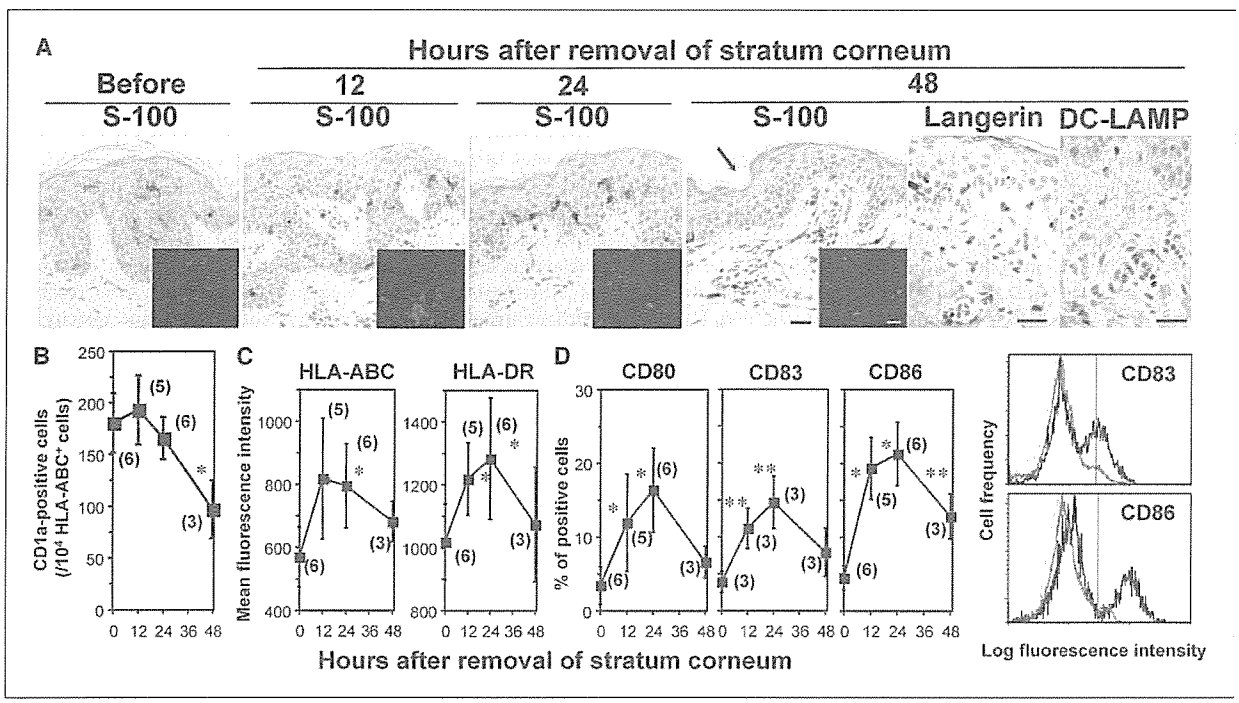

Figure 1. Kinetics of LCs and expression of HLA and costimulatory molecules on LCs in relation to removal of the SC. Skin samples from normal individuals were examined before, 12, 24, and 48 hours after removal of the SC. The numbers in parentheses indicate the number of subjects that participated. *A*, $S\text{-}100^+$, Langerin/$CD207^+$ and DC-LAMP/$CD208^+$ cells (*brown*) in the skin samples immunostained with a standard avidin-biotin complex method. Nuclear counterstaining was achieved with hematoxylin. *Arrow*, regenerating SC. *Insets*, composite confocal images of epidermal sheets showing HLA-DR^+ cells. Representative sections are shown. *Bar*, 50 μm. *B*, enumeration of $CD1a^+$ cells in HLA-ABC^+ epidermal cells. *Points*, mean; *bars*, ±SD. *C* and *D*, expression profiles of HLA-ABC, HLA-DR, CD80, CD83, and CD86 in epidermal LCs. *C*, mean fluorescence intensity was determined as a linear scale (0-1,020). *D*, percentage of positive cells in LC populations were determined. LCs were separated from contaminating epidermal cells using FL2-gate settings as PE-labeled $CD1a^+$ cells and FL3-gate settings as PerCP-labeled HLA-DR^+ cells, as well as forward scatter/side scatter gating. The viability of the cells within this gate was always >95% as determined by the addition of propidium iodide to each sample. Representative flow cytometric analyses of cell surface CD83 and CD86 expression before (*red lines*) and 24 hours after (*black lines*) the barrier disruption. Cells stained with isotype control antibody (*green lines*). *Points*, mean; *bars*, ±SD; *, $P < 0.01$; **, $P < 0.05$, as compared with no treatment (0 hours).

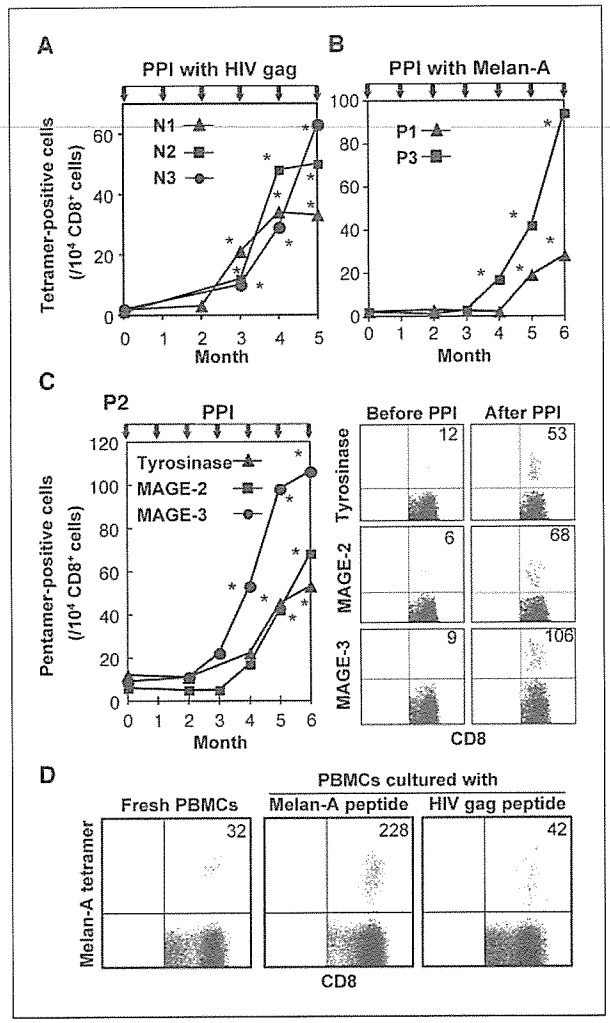

Figure 2. Induction of peptide-specific, tetramer-positive, and pentamer-positive $CD8^+$ T cells. PBMCs obtained 7 days after each PPI were immunophenotyped with the HIV gag-tetramer in N1 to N3 (*A*), Melan-A-tetramer in P1 and P3 (*B*), and pentamers for tyrosinase, MAGE-2, and MAGE-3 in P2 (*C*), and analyzed by flow cytometry. Alternatively, cells were cultured with Melan-A or HIV gag peptide for 5 days and subjected to tetramer binding assay (*D*). *A*, kinetics of HIV gag tetramer-positive cells. The value for HIV gag-specific cells/10^4 $CD8^+$ cells in HLA-A*0201 control subjects (n = 6) without PPI was 1.83 ± 0.75 (mean ± SD). *,+2 SD above the mean. *B* and *C*, kinetics of tetramer/pentamer-positive cells in melanoma patients. The number of Melan-A-specific cells/10^4 $CD8^+$ cells in HLA-A*0201 control subjects (n = 6) without PPI was 2.50 ± 1.05 (mean ± SD). The number of tyrosinase-, MAGE-2-, and MAGE-3-specific cells/10^4 $CD8^+$ cells in HLA-A*24 control subjects (n = 6) without PPI were 10.2 ± 5.9, 11.3 ± 5.0, and 15.6 ± 3.8, respectively (mean ± SD). *,+2 SD above the mean. *D*, specificity of tetramer-positive cell induction by PPI. Results of a representative experiment for cells after the seventh immunization with Melan-A from P1. Numbers are tetramer-positive cells/10^4 $CD8^+$ cells. Tetramer-positive cells in cultures stimulated with nonimmunizing peptide were always below the mean +2 SD of control subjects (n = 6).

diameters of five target lesions selected before PPI (Fig. 4*B*). In P7, a small s.c. nodule, with the longest diameter at 2 cm, disappeared. In P8, the intensities of the scintigraphic signals in five of six multiple bone metastases were attenuated after PPI (Fig. 4*C*). In accordance with these findings, the level of serum 5-S-cysteinyl-dopa was reduced from 27 nmol/L before PPI to 4.2 nmol/L after PPI (normal, <8.0 nmol/L). In P4 and P6, the melanoma invasion progressed rapidly, despite CTL induction, and both patients died of the tumor within 4 months of PPI completion. In P2 and P7, although skin nodules had developed at frequencies of one and three per 2 months, respectively, and been dissected during the 6 months prior to PPI, new lesions did not appear for 6 months during PPI. These patients developed several new lesions at

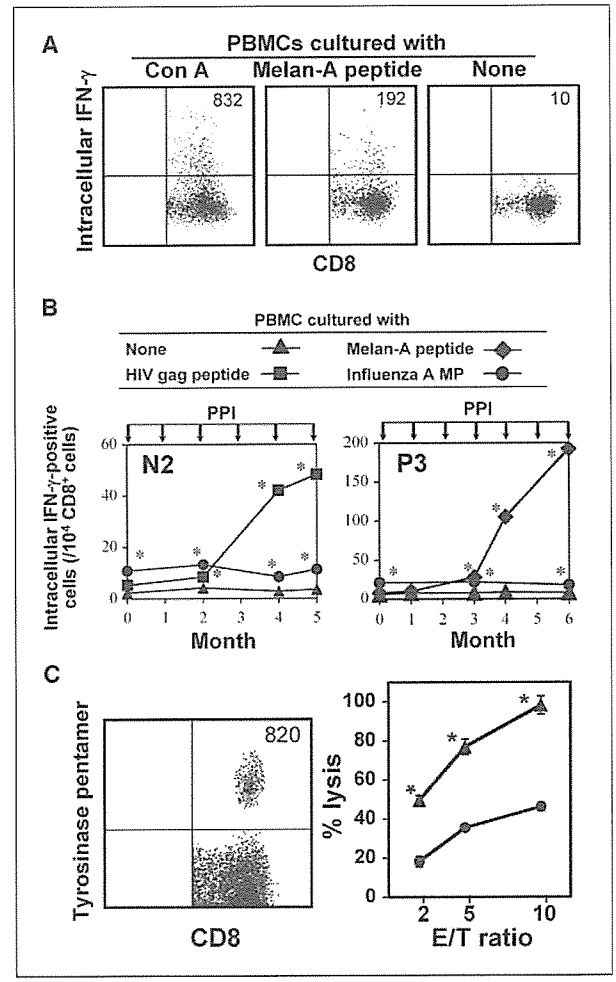

Figure 3. Induction of an intracellular IFN-γ^+ $CD8^+$ T cell response by PPI. PBMCs obtained 7 days after PPI were cultured with either HIV gag, Melan-A, influenza A MP, or Con A for 48 hours depending on the experiment purpose and subjected to intracellular IFN-γ assay. *A*, specific induction of intracellular IFN-γ-positive cells by PPI. Results of a representative experiment in P3 after the seventh immunization. Numbers indicate IFN-γ^+ cells/10^4 $CD8^+$ T cells. In the Con A culture, these were 320 in N1, 343 in N2, 425 in N3, and 892 in P1. *B*, kinetics of peptide-specific T cells producing IFN-γ. Results of representative experiments in N2 and P3. Immunizing peptide was HIV gag in N2 and Melan-A in P3. The number of HIV gag–specific cells/10^4 $CD8^+$ cells in HLA-A*0201 control subjects (n = 6) without PPI was 3.86 ± 1.77 (mean ± SD). The number of Melan-A-specific cells/10^4 $CD8^+$ cells in HLA-A*0201 control subjects (n = 5) without PPI was 4.17 ± 1.60 (mean ± SD). *,+2 SD above the mean. *C*, results of representative *in vitro* peptide-dependent cytolytic experiments in P2. PBMCs at completion of PPI were stimulated with tyrosinase and subjected to CTL assay in the presence of T2-A24 target cells loaded with (▲) or without (●) the peptide. Effector cell populations contained 820 tyrosinase pentamer-positive cells/10^4 $CD8^+$ cells as shown in a flow cytometric profile. *Points,* mean of triplicate cultures; *bars,* ±SD. *, $P < 0.01$ as compared with lysis of T2-A24 cells not loaded with the relevant peptide. *E/T ratio,* effector-to-target ratio.

3 to 5 months after completion of PPI, once the number of circulating CTLs had dropped to less than half the peak value (data not shown). The fact that P2 and P7 were free from melanoma lesions for 9 to 11 months during and after PPI suggested the suppressive effect of this procedure on tumor development. Therefore, the clinical outcomes in this small pilot study clearly suggest the beneficial effects of PPI for patients with advanced melanoma.

Migration of CTLs into melanoma lesions after PPI. Skin tissue specimens were available in association with PPI for P2 and P4, and subjected to histologic and immunohistochemical examinations as well as flow cytometric analysis. In P4, in whom the melanoma progressed despite CTL induction in the blood, there was no lymphoid cell infiltration before or after PPI (Fig. 5*A*, *a*). In P2, the metastatic lesions contained no cellular infiltrate before the first round of PPI (Fig. 5*A*, *b*). This patient received a second round of PPI due to the development of three new lesions at 3 months after completion of the first round of PPI. After the second immunization in the second round, the regressing lesions showed marked lymphoid cell infiltration and apoptotic and necrotic melanoma cells (Fig. 5*A*, *c* and *d*). $CD8^+$ cells had infiltrated the tumor mass and $CD4^+$ cells were located at the periphery of the lesions (Fig. 5*A*, *e* and *f*). Flow cytometric analysis revealed that the tumor-infiltrating leukocytes contained $CD4^+$ cells and $CD8^+$ cells in equal proportions (Fig. 5*B*). Furthermore, 9.8%, 8.4%, and 12.7% of the cells among the $CD8^+$ tumor-infiltrating cells were positive for tyrosinase, MAGE-2, and MAGE-3 pentamers, respectively (Fig. 5*B*). The proportions of tyrosinase, MAGE-2, and MAGE-3 pentamer–positive cells in the circulation at this time were 0.42%, 0.52%, and 0.8% of the $CD8^+$ cells, respectively, indicating selective migration of peptide-specific CTLs into the melanoma lesions.

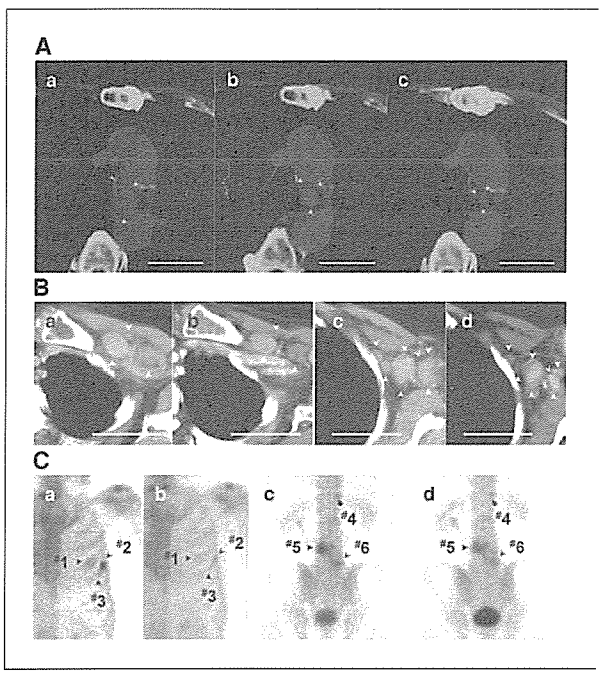

Figure 4. Clinical efficacy of PPI for melanoma treatment. *A*, computed tomography scans of a mediastinal lymph node (*arrowheads*) in P3 on entry (*a*), after the fourth PPI (*b*), and at completion of PPI (*c*). *B*, multiple metastatic lesions (*arrowheads*) in the left upper chest (*a* and *b*) and left axilla (*c* and *d*) in P5 on entry (*a* and *c*) and at completion of PPI (*b* and *d*). *C*, ^{99m}Tc-bone scintigraphs of metastatic bone lesions (#1-#6) in P8 before (*a* and *c*) and after (*b* and *d*) PPI. P3 presented with a melanoma lesion on the left palpebral conjunctiva and received orbital exenteration and wide local excision 15 years previously. Metastatic lesions appeared on the skin of the neck and the left parotid gland >12 years after the previous treatment. Despite total excision of the recurrent lesions and postoperative combination adjuvant therapy, metastases developed in mediastinal lymph nodes 3 months before entry. P5 underwent excision of primary skin lesions 5 years previously without any subsequent treatment, and developed multiple s.c. metastatic tumors at 5 months before entry. P8 had multiple bone metastases, as detected by bone scintigraphy, despite the resection of a lesion of the first toe of the right foot and right inguinal metastatic lymph nodes, and subsequent chemotherapy 2 years before entry.

Laboratory findings and untoward clinical features. Repeated assessment of hemograms and liver and renal functions revealed no abnormalities during and at completion of PPI in normal participants and the patients except P4. Results of the laboratory examination were normal during the 1-year follow-up period after completion of PPI in N1 to N3. Liver functions progressively deteriorated during PPI and until death in P4 because of multiple liver metastases. N1 to N3 developed no physical signs of autoimmunity, and rheumatoid factors or autoantibodies including antinuclear antibodies were negative 1 year after PPI. Generalized progressive vitiligo spots developed in P1, P3, P5, and P6 after several immunizations, although no other physical signs or serologic findings of autoimmunity were detected at completion of PPI.

Follow-up. P1 and P3 were disease-free for 15 to 19 months after the first round of PPI. New small s.c. nodules in P2 and P7, which developed at 3 and 5 months, respectively, after the first round of PPI, disappeared after a second round of PPI. Despite the regression of the initial target lesions at the end of PPI, P5 developed new s.c. and metastatic lesions while undergoing monthly immunization in succession to the PPI due to the patient's request. P8 developed a new bone lesion with an increase in the serum 5-S-cysteinyldopa level at 4 months after PPI, although the densities of the previous bone lesions remained decreased, as evaluated by scintigraphy.

Discussion

The present study showed that PPI, a novel immunization protocol for peptide application to barrier-disrupted skin, induces potent CTL responses and provides a promising approach for cancer therapy in human beings. Because an adjuvant effect seems to be inherent in perturbation of the skin integrity (21), the hallmark of PPI is that it closely mimics the natural trigger of DC activation, conducive to CTL expansion as fully activated effector cells. Although only a part (a maximum of 20%) of LCs were actually activated, the main and effective inducer of CTL would be LCs, considering their *in situ* kinetics after removal of SC in human and the augmented CTL priming capacity of LCs in barrier-disrupted murine skin (20). Recent studies in murine herpes virus infection models (34, 35), as well as novel mouse systems in which LCs can be selectively removed/ablated (36–38), have suggested that skin-resident APCs other than LCs contribute in the generation of immune responses *in vivo*. Therefore, it was possible that these cell types also participated in peptide-specific CTL immunity in the current protocol. Individual differences in the LC emigration profile of these APCs through skin and the amount of peptide absorbed via barrier-disrupted skin may be one critical factor in determining the timing and magnitude of CTL responses. An important issue is the demonstration of an actual therapeutic or preventive application of PPI in humans. In fact, the pilot study revealed a beneficial effect of PPI on the growth inhibition of

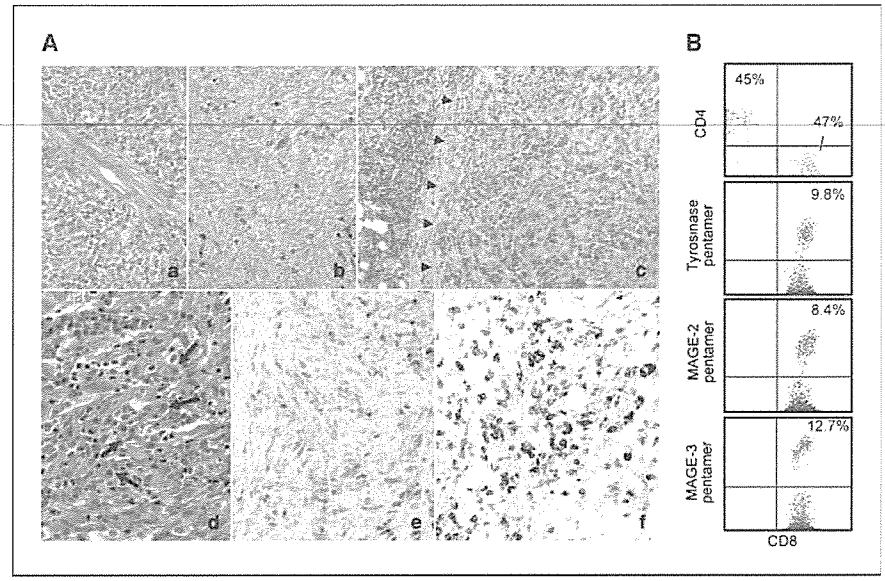

Figure 5. *In vivo* infiltration of CTLs into melanoma lesions induced by PPI. *A,* H&E histology and immunohistology of metastatic skin lesions. Skin lesions from P4 after PPI (*a,* magnification, ×200), from P2 before (*b,* magnification, ×200) and after PPI (*c, arrowheads,* tumor mass; magnification, ×100), with apoptotic and necrotic cells (*d, arrows*; magnification, ×400) and immunohistochemical staining showing infiltration of $CD4^+$ cells (*e,* magnification, ×100) and $CD8^+$ cells (*f,* magnification, ×100). *B,* flow cytometric profiles of cell suspensions obtained from a regressing s.c. nodule in P2 during PPI, showing the percentage of $CD4^+$ and $CD8^+$ cells among $CD45^+$ cell-gated leukocytes and the percentage of pentamer$^+$ cells among the $CD8^+$ $CD45^+$ cell-gated populations.

tumors in patients with advanced melanoma, which accompanied the induction of specific CTL activity. None of the patients/controls who received PPI exhibited local or systemic toxicity, or developed any clinical and laboratory findings of autoimmunity except vitiligo in patients with melanoma. We therefore propose that this novel strategy is clinically relevant for application in the treatment of malignancies. Furthermore, the generation of HIV gag–specific CTLs indicates the prophylactic strategy of PPI against viral and helminth infections.

Methods of needle-free vaccination delivery have attracted a global interest because of the urgent need for eradication of pandemic disease and treatment of growing numbers of cancer patients. This new approach has several advantages regarding ease and speed of delivery, safety and compliance, and costs, over needle delivery. Reported needle-free strategies to manipulate primarily the skin immune system include transcutaneous immunization (TCI; refs. 19, 39, 40), penetration via hair follicles (41), cutaneous bombardment (42), epidermal powder immunization (43, 44), and immunization with microenhancer arrays (45). All of these protocols target antigen to skin DCs in association with their activation and emigration from the skin, regulating the magnitudes, types, and directions of the immune responses. In particular, TCI is close to PPI in the methodologic respect. Both TCI and PPI are characterized by the application of antigen to the skin surface, thereby treating pathologic processes at a location distant from the application site. The difference between these two methods is the use of adjuvant. To obtain satisfactory immune responses, TCI requires adjuvant such as cholera toxin added to a vaccine antigen. On the other hand, barrier disruption is mandatory to allow the antigen to penetrate and activate the skin immune system in PPI without adjuvant. Although comparison of the effectiveness of CTL induction between PPI and other transcutaneous methods is difficult at present, the current study is the first one that clearly shows the clinical efficacy of PPI-induced CTLs in the human system.

Among many variables in the protocols and technologies of DC immunotherapy, quality control of vaccines in relation to the maturation status of DCs is a key determinant for the regulation of immune responses, and thus, clinical efficacy (4). Barrier disruption with the strong glue in PPI constantly removed a definite amount of the horny layers, irrespective of age, gender, and treated sites of the recipient. Such reproducibility of barrier perturbation enabled us to use *in situ* activated and fully matured LCs as therapeutic vectors. Repeated manipulations were essential to induce CTL responses with clinical efficacy in PPI as in prevailing melanoma vaccine with DC preparations (6). Such a time-consuming strategy might pose a problem when rapid protective responses are required. The application of appropriate adjuvants to the sites of barrier disruption has been shown to enhance immune responses both in mice (19, 39) and in humans (40). Systemic and local incorporation of T cell adjuvants such as interleukin-2, IFNs, and CD4 epitopes to PPI may potentiate CTL induction with less frequent immunization.

In the present pilot study, PPI was in fact effective in patients with advanced melanoma because tumor size was reduced in four of six patients, and apparent tumor burden and tumor development seemed to be abrogated in another. These beneficial effects coincided with the emergence of CTLs with strong cytolytic activity in the blood of some patients. Regressing lesions following PPI was associated with preferential infiltration of CTLs in a responder patient. In contrast, one patient with multiple metastases, and another with primary esophageal melanoma, did not clinically respond to PPI despite the presence of circulating CTLs. The possible reasons for treatment failure seemed to be related to the lack of cellular infiltrate in lesions and the impaired ability of CTLs to propagate *in vitro* under antigenic stimulation. A variety of immunologic mechanisms to evade tumor cell killing might underlie such T cell defects in these patients (46–48).

The safety issue is an important concern because the development of autoimmunity has been reported with the introduction of antigens directly into the body (49). Vitiligo, a well-known feature of autoimmunity targeting melanocytes, develops in association with DC-based immunotherapy in melanoma cases (49, 50). Because the antigens used for the immunization are autoantigens, there would be no expectation of epitope spreading. Although no study participants undergoing PPI

showed any signs of autoimmunity other than vitiligo, careful and repeated follow-up of the recipient's physical condition is indispensable for clinical trials.

Acknowledgments

Received 3/20/2006; revised 7/17/2006; accepted 7/31/2006.

Grant support: Ministry of Education, Science, Sports, and Culture of Japan (Grant-in-Aid for Scientific Research, 13670878 to H. Yagi and 13470170 to M. Takigawa).

The costs of publication of this article were defrayed in part by the payment of page charges. This article must therefore be hereby marked *advertisement* in accordance with 18 U.S.C. Section 1734 solely to indicate this fact.

We are indebted to Drs. K. Kuzushima, Department of Tumor Immunology, Aichi Cancer Center, Aichi, Japan, for providing T2-A24 cells; T. Nishijima, Kao Corporation, Haga, Japan; and S. Inoue, Kanebo Cosmetics Inc., Odawara, Japan for assistance with the TEWL measurements. The technical assistance of K. Sugaya is also gratefully acknowledged.

References

1. Hsu FJ, Benike C, Fagnoni F, et al. Vaccination of patients with B-cell lymphoma using autologous antigen-pulsed dendritic cells. Nat Med 1996;2:52–8.
2. Kundu SK, Dupuis M, Sette A, et al. Role of preimmunization virus sequences in cellular immunity in HIV-infected patients during HIV type 1 MN recombinant gp160 immunization. AIDS Res Hum Retroviruses 1998;14:1669–78.
3. Nestle FO, Alijagic S, Gilliet M, et al. Vaccination of melanoma patients with peptide- or tumor lysate-pulsed dendritic cells. Nat Med 1998;4:328–32.
4. Dhodapkar MV, Steinman RM. Antigen-bearing immature dendritic cells induce peptide-specific $CD8^+$ regulatory T cells *in vivo* in humans. Blood 2002;100:174–7.
5. Dhodapkar MV, Krasovsky J, Steinman RM, Bhardwaj N. Mature dendritic cells boost functionally superior $CD8^+$ T-cell in humans without foreign helper epitopes. J Clin Invest 2000;105:R9–14.
6. Paczesny S, Banchereau J, Wittkowski KM, Saracino G, Fay J, Palucka AK. Expansion of melanoma-specific cytolytic $CD8^+$ T cell precursors in patients with metastatic melanoma vaccinated with $CD34^+$ progenitor-derived dendritic cells. J Exp Med 2004;199:1503–11.
7. Schuler-Thurner B, Schultz ES, Berger TG, et al. Rapid induction of tumor-specific type 1 T helper cells in metastatic melanoma patients by vaccination with mature, cryopreserved, peptide-loaded monocyte-derived dendritic cells. J Exp Med 2002;195:1279–88.
8. Banchereau J, Schuler-Thurner B, Palucka AK, Schuler G. Dendritic cells as vectors for therapy. Cell 2001;106:271–4.
9. Jonuleit H, Giesecke-Tuettenberg A, Tuting T, et al. A comparison of two types of dendritic cell as adjuvants for the induction of melanoma-specific T-cell responses in humans following intranodal injection. Int J Cancer 2001;93:243–51.
10. de Vries IJ, Krooshoop DJ, Scharenborg NM, et al. Effective migration of antigen-pulsed dendritic cells to lymph nodes in melanoma patients is determined by their maturation state. Cancer Res 2003;63:12–7.
11. de Vries IJ, Lesterhuis WJ, Scharenborg NM, et al. Maturation of dendritic cells is a prerequisite for inducing immune responses in advanced melanoma patients. Clin Cancer Res 2003;9:5091–100.
12. Figdor CG, de Vries IJ, Lesterhuis WJ, Melief CJ. Dendritic cell immunotherapy: mapping the way. Nat Med 2004;10:475–80.
13. Engleman EG. Dendritic cell-based cancer immunotherapy. Semin Oncol 2003;30:23–9.
14. Jakob T, Udey MC. Epidermal Langerhans cells: from neurons to nature's adjuvants. Adv Dermatol 1999;14:209–58.
15. Banchereau J, Briere F, Caux C, et al. Immunobiology of dendritic cells. Annu Rev Immunol 2000;18:767–811.
16. Raz E, Carson DA, Parker SE, et al. Intradermal gene immunization: the possible role of DNA uptake in the induction of cellular immunity to viruses. Proc Natl Acad Sci U S A 1994;91:9519–23.
17. Bouloc A, Walker P, Grivel JC, Vogel JC, Katz SI. Immunization through dermal delivery of protein-encoding DNA: a role for migratory dendritic cells. Eur J Immunol 1999;29:446–54.
18. Granstein RD, Ding W, Ozawa H. Induction of anti-tumor immunity with epidermal cells pulsed with tumor-derived RNA or intradermal administration of RNA. J Invest Dermatol 2000;114:632–6.
19. Belyakov IM, Hammond SA, Ahlers JD, Glenn GM, Berzofsky JA. Transcutaneous immunization induces mucosal CTLs and protective immunity by migration of primed skin dendritic cells. J Clin Invest 2004;113:998–1007.
20. Seo N, Tokura Y, Nishijima T, Hashizume H, Furukawa F, Takigawa M. Percutaneous peptide immunization via corneum barrier-disrupted murine skin for experimental tumor immunoprophylaxis. Proc Natl Acad Sci U S A 2000;97:371–6.
21. Nishijima T, Tokura Y, Imokawa G, Seo N, Furukawa F, Takigawa M. Altered permeability and disordered cutaneous immunoregulatory function in mice with acute barrier disruption. J Invest Dermatol 1997;109:175–82.
22. Godefroy S, Peyre M, Garcia N, Muller S, Sesardic D, Partidos CD. Effect of skin barrier disruption on immune responses to topically applied cross-reacting material, CRM197, of diphtheria toxin. Infect Immun 2005;73:4803–9.
23. Nagatani T, Ichiyama S, Onuma R, et al. The use of DAV (DTIC, ACNU and VCR) and natural interferon-β combination therapy in malignant melanoma. Acta Derm Venereol 1995;75:494.
24. Sliz P, Michielin O, Cerottini JC, et al. Crystal structures of two closely related but antigenically distinct HLA-A2/melanocyte-melanoma tumor-antigen peptide complexes. J Immunol 2001;167:3276–84.
25. Yagi H, Tokura Y, Furukawa F, Takigawa M. Th2 cytokine mRNA expression in primary cutaneous CD30-positive lymphoproliferative disorders: successful treatment with recombinant interferon-γ. J Invest Dermatol 1996;107:827–32.
26. Cooper KD, Fox P, Neises G, Katz SI. Effects of ultraviolet radiation on human epidermal cell alloantigen presentation: initial depression of Langerhans cell-dependent function is followed by the appearance of T6− Dr+ cells that enhance epidermal alloantigen presentation. J Immunol 1985;134:129–37.
27. Yu RC, Abrams DC, Alaibac M, Chu AC. Morphological and quantitative analyses of normal epidermal Langerhans cells using confocal scanning laser microscopy. Br J Dermatol 1994;131:843–8.
28. Yagi H, Tokura Y, Wakita H, Furukawa F, Takigawa M. $TCRV\beta7^+$ Th2 cells mediate UVB-induced suppression of murine contact photosensitivity by releasing IL-10. J Immunol 1996;156:1824–31.
29. Hashizume H, Takigawa M, Tokura Y. Characterization of drug-specific T cells in phenobarbital-induced eruption. J Immunol 2002;168:5359–68.
30. Kuzushima K, Hayashi N, Kimura H, Tsurumi T. Efficient identification of HLA-A*2402-restricted cytomegalovirus-specific $CD8^+$ T-cell epitopes by a computer algorithm and an enzyme-linked immunospot assay. Blood 2001;98:1872–81.
31. Seo N, Hayakawa S, Takigawa M, Tokura Y. Interleukin-10 expressed at early tumour sites induces subsequent generation of $CD4^+$ T-regulatory cells and systemic collapse of antitumour immunity. Immunology 2001;103:449–57.
32. Therasse P, Arbuck SG, Eisenhauer EA, et al. New guidelines to evaluate the response to treatment in solid tumors. J Natl Cancer Inst 2000;92:205–16.
33. Lutz MB, Schuler G. Immature, semi-mature and fully mature dendritic cells: which signals induce tolerance or immunity? Trends Immunol 2002;23:445–8.
34. Allan RS, Smith CM, Belz GT, et al. Epidermal viral immunity induced by $CD8\alpha^+$ dendritic cells but not by Langerhans cells. Science 2003;301:1925–8.
35. Zhao X, Deak E, Soderberg K, et al. Vaginal submucosal dendritic cells, but not Langerhans cells, induce protective Th1 responses to herpes simplex virus-2. J Exp Med 2003;197:153–62.
36. Bennett CL, van Rijn E, Jung S, et al. Inducible ablation of mouse Langerhans cells diminishes but fails to abrogate contact hypersensitivity. J Cell Biol 2005;169:569–76.
37. Kaplan DH, Jenison MC, Saeland S, Shlomchik WD, Shlomchik MJ. Epidermal Langerhans cell-deficient mice develop enhanced contact hypersensitivity. Immunity 2005;23:611–20.
38. Kissenpfennig A, Henri S, Dubois B, et al. Dynamics and function of Langerhans cells *in vivo*: dermal dendritic cells colonize lymph node areas distinct from slower migrating Langerhans cells. Immunity 2005;22:643–54.
39. Guebre-Xabier M, Hammond SA, Epperson DE, Yu J, Ellingsworth L, Glenn GM. Immunostimulant patch containing heat-labile enterotoxin from *Escherichia coli* enhances immune responses to injected influenza virus vaccine through activation of skin dendritic cells. J Virol 2003;77:5218–25.
40. Frech SA, Kenney RT, Spyr CA, et al. Improved immune responses to influenza vaccination in the elderly using an immunostimulant patch. Vaccine 2005;23:946–50.
41. Fan H, Lin Q, Morrissey GR, Khavari PA. Immunization via hair follicles by topical application of naked DNA to normal skin. Nat Biotechnol 1999;17:870–2.
42. Morel PA, Falkner D, Plowey J, Larregina AT, Falo LD, Jr. DNA immunisation: altering the cellular localisation of expressed protein and the immunisation route allows manipulation of the immune response. Vaccine 2004;22:447–56.
43. Roy MJ, Wu MS, Barr LJ, et al. Induction of antigen-specific CD8+ T cells, T helper cells, and protective levels of antibody in humans by particle-mediated administration of a hepatitis B virus DNA vaccine. Vaccine 2000;19:764–78.
44. Chen D, Payne LG. Targeting epidermal Langerhans cells by epidermal powder immunization. Cell Res 2002;12:97–104.
45. Mikszta JA, Alarcon JB, Brittingham JM, Sutter DE, Pettis RJ, Harvey NG. Improved genetic immunization via micromechanical disruption of skin-barrier function and targeted epidermal delivery. Nat Med 2002;8:415–9.
46. Chouaib S, Asselin-Paturel C, Mami-Chouaib F, Caignard A, Blay JY. The host tumor immune conflict: from immunosuppression to resistance and destruction. Immunology Today 1997;18:493–7.
47. Strand S, Galle PR. Immune evasion by tumours: involvement of the CD95 (APO-1/Fas) system and its clinical implications. Mol Med Today 1998;4:63–8.
48. Ko EC, Wang X, Ferrone S. Immunotherapy of malignant diseases. Challenges and strategies. Int Arch Allergy Immunol 2003;132:294–309.
49. Gilboa E. The risk of autoimmunity associated with tumor immunotherapy. Nat Immunol 2001;2:789–92.
50. Lane C, Leitch J, Tan X, Hadjati J, Bramson JL, Wan Y. Vaccination-induced autoimmune vitiligo is a consequence of secondary trauma to the skin. Cancer Res 2004;64:1509–14.

Novel ALDH3A2 Heterozygous Mutations in a Japanese Family with Sjögren–Larsson Syndrome

Journal of Investigative Dermatology (2006) **126,** 2545–2547. doi:10.1038/sj.jid.5700453; published online 22 June 2006

TO THE EDITOR

Sjögren–Larsson syndrome (SLS: OMIM No. 270200) is an autosomal-recessive hereditary disorder characterized by congenital ichthyosis, mental retardation, and spastic diplegia or tetraplegia (Rizzo, 1993). Rizzo *et al.* (1988) revealed that long-chain fatty alcohol was abnormally accumulated in cultured fibroblasts, white blood cells and serum in SLS patients. In 1996, De Laurenzi *et al.* (1996) reported that mutations in the fatty aldehyde dehydrogenase (FALDH) gene (*ALDH3A2*) underlie SLS. In the present study, we report novel compound heterozygous mutations in *ALDH3A2* in a Japanese family with SLS.

A 2-year-old Japanese girl was suffering from congenital ichthyosis, mental retardation, spastic tetraplegia, and recurrent epileptic seizures. The patient was the first child of non-consanguineous, healthy Japanese parents. Ichthyosis was not seen in any other family members. She was born as a pre-term baby at 34 weeks 3 days of gestation (body weight, 2392 g), but not a collodion baby. Physical examination revealed fine scales and slight erythema over her whole body (Figure 1). Hyperkeratosis was also seen on the palms and soles. Her hair, nails, and teeth were normal. The skin manifestations were consistent with non-bullous congenital ichthyosiform erythroderma. Her extremities were hypertonic. T2-weighted magnetic resonance imaging demonstrated a high-intensity area in her brain periventricular white matter. Ophthalmologic examination revealed retinal crystals, generally referred to as "glistening white dots".

To elucidate the precise genetic abnormality in the family, mutational analysis was performed in the affected girl and her parents. Briefly, genomic DNA isolated from peripheral blood cells was subjected to PCR amplification, followed by direct automated sequencing using an ABI PRISM 3100 genetic analyzer (ABI Advanced Biotechnologies, Columbia, MD). Oligonucleotide primers and PCR conditions used for amplification of all exons and exon–intron borders of *ALDH3A2* were originally derived from the report by Rizzo *et al.* (1999) and were partially modified for our study (Shibaki *et al.*, 2004). The entire coding region including the intron/exon boundaries for both forward and reverse DNA strands from the patient, her parents and 100 healthy Japanese controls were sequenced. In the patient, a combination of two novel heterozygous mutations, 332G>A in exon 2 and 636T>G in exon 4, were identified (Figure 2a). The mutation 332G>A was present in her father, and the mutation 636T>G was demonstrated in her mother. The presence of both mutations was excluded in 200 alleles of 100 normal unrelated Japanese individuals. The medical ethical committee of the Hokkaido University approved all described studies. These studies were conducted according to the Declaration of Helsinki Principles. The patient's parents gave their written informed consent.

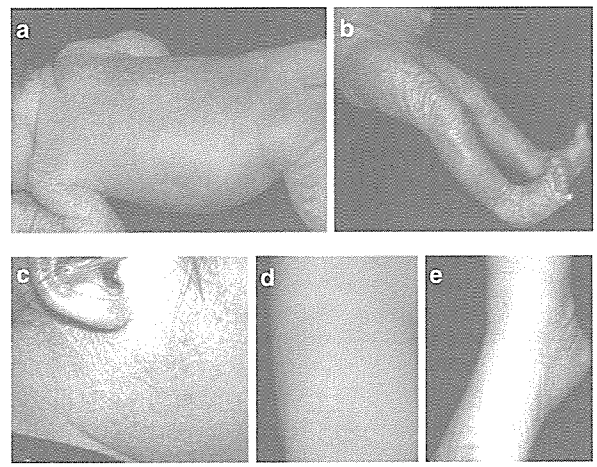

Figure 1. **Clinical features of the SLS patient. (a, b)** In the perinatal period, xerotic skin, and fine scales were apparent over the (**a**) proband's trunk and (**b**) hyperkeratosis was severe on her legs. (**c, d, e**) At 2 years of age, fine, whitish scales were seen on her (**c**) cheek, (**d**) thigh, and the (**e**) dorsal foot.

The paternal mutation 332G>A in exon 2 leads to an alteration of the tryptophan residue at codon 111 into a stop codon (nonsense mutation W111X) and this premature translation termination eliminates approximately 80% of the length of FALDH polypeptide (loss of 77.3% length of the FALDH major splice variant). Thus, this nonsense mutation is expected to seriously abolish FALDH function.

The maternal mutation 636T>G in exon 4 resulted in an alteration of a serine at codon 212 to arginine (S212R). FALDH amino-acid sequence alignment shows that this serine residue at codon 212 is conserved among several diverse species (reference sequences: CR457422, XP 511337, NP 113919, CAI25890, NP 001016537, AAK49120) (Figure 2b).

In addition, according to a comparison of 145 full-length aldehyde dehydrogenase-related sequences by Perozich *et al.* (1999), this serine is

Abbreviations: FALDH, fatty aldehyde dehydrogenase; SLS, Sjögren–Larsson syndrome

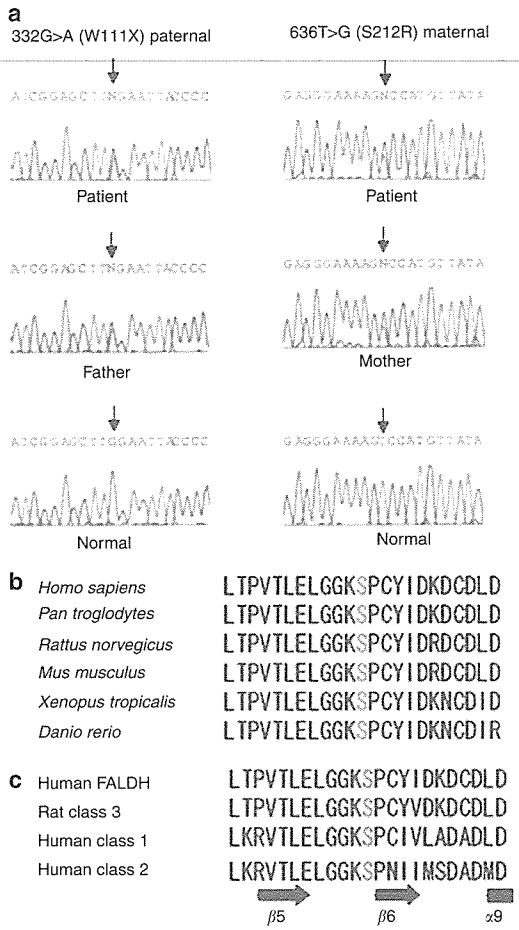

Figure 2. *ALDH3A2* mutations in the present SLS patient and sequence alignments around the missense mutation. (**a**) Sequence analysis of the *ALDH3A2*. A combination of heterozygous mutations derived from their mother (332G>A (W111X) in exon 2) and father (636T>G (S212R) were detected. (**b**) FALDH amino-acid sequence alignment shows the level of conservation in diverse species of the amino-acid S212 (red characters), which was altered by the missense mutation in the present family. (**c**) A sequence alignment between the FALDH, rat class 3 and human class 1 and class 2 ALDHs showing the relative locations of key residues in these enzymes. Serine residue at codon 212 of FALDH is strictly conserved. Secondary structure components found in the class 3 rat ALDH structure are presented with a bar and arrows. The bar represents an α-helix and arrows represent β-strands. (Modified from the paper by Liu *et al.*, (1997).)

highly conserved among many of the ALDH family members, and participates in one of the 10 most conserved sequence motifs in ALDHs (Figure 2c). In addition, analysis of the crystallized three-dimensional structure of the related class 3 rat cytosolic ALDH revealed that this serine is located adjacent to the first β-strand, β6, of the six parallels of β-strands, comprising a significant portion of the catalytic domain of the molecule (Liu *et al.*, 1997) (Figure 2c). These findings strongly suggest that the serine at codon 212 is important for connecting the α/β structure of a dinucleotide-binding Rossmann fold (Freshney *et al.*, 1994) to the catalytic domain and/or for structural folding of the catalytic domain, and is therefore essential for the normal function of the FALDH protein. The fact that the present patient harboring the missense mutation S212R showed typical SLS phenotypic features strongly suggests that this serine residue is essential for FALDH enzymatic function.

FALDH is a microsomal NAD-dependent enzyme, which is necessary for the oxidation of long-chain aliphatic aldehydes into fatty acids (Kelson *et al.*, 1997). The FALDH gene (*ALDH3A2*) located on chromosome 17p11.2 (De Laurenzi *et al.*, 1996) comprises 11 exons, and is widely expressed in a variety of tissues (Chang and Yoshida, 1997; Rogers *et al.*, 1997). Until now, a number of mutations in *ALDH3A2* have been shown to be responsible for SLS over the world (Rizzo *et al.*, 1999). Founder effects were observed in certain areas and races (Rizzo *et al.*, 1999; Kraus *et al.*, 2000; Rizzo and Carney, 2005). In Japanese patients with SLS, one homozygous mutation 1157A>G (N386S) in *ALDH3A2* was reported in a patient of one family (Aoki *et al.*, 2000) and two other mutations, 481delA and 1087_1089delGTA, were reported in another family (Shibaki *et al.*, 2004). We have detected two additional mutations, 332G>A (W111X) and 636T>G (S212R), in the present family. All the mutations detected in Japanese families were distinct one another and we therefore speculate there is no founder effect in Japanese cases with *ALDH3A2* mutations causing SLS.

The pathogenesis of the ichthyosis in SLS includes abnormal lamellar or membranous inclusions in cornified cells, which were reported in a patient with SLS, although causative genetic abnormalities were not known in that particular case (Ito *et al.*, 1991). The inclusions were speculated to be lamellar granule-in-origin. Later, a deficiency in acyl-ceramides in the lipid layer in the stratum corneum was also reported in SLS patients (Paige *et al.*, 1994). In a previous report (Shibaki *et al.*, 2004), we observed ultrastructurally abnormal lamellar granules lacking normal lamellar contents in the upper spinous and granular layers. In addition, we showed some malformed lamellar granule components were secreted into the intercellular space in the stratum corneum (Shibaki *et al.*, 2004). These observations suggest defective lamellar granule formation in SLS. SLS is thought to be a form of ichthyoses caused by defective